

A model of annular linear induction pumps

Nuclear Engineering Division

About Argonne National Laboratory

Argonne is a U.S. Department of Energy laboratory managed by UChicago Argonne, LLC under contract DE-AC02-06CH11357. The Laboratory's main facility is outside Chicago, at 9700 South Cass Avenue, Argonne, Illinois 60439. For information about Argonne and its pioneering science and technology programs, see www.anl.gov.

DOCUMENT AVAILABILITY

Online Access: U.S. Department of Energy (DOE) reports produced after 1991 and a growing number of pre-1991 documents are available free via DOE's SciTech Connect (<http://www.osti.gov/scitech/>)

Reports not in digital format may be purchased by the public from the National Technical Information Service (NTIS):

U.S. Department of Commerce
National Technical Information Service
5301 Shawnee Rd
Alexandria, VA 22312
www.ntis.gov
Phone: (800) 553-NTIS (6847) or (703) 605-6000
Fax: (703) 605-6900
Email: orders@ntis.gov

Reports not in digital format are available to DOE and DOE contractors from the Office of Scientific and Technical Information (OSTI):

U.S. Department of Energy
Office of Scientific and Technical Information
P.O. Box 62
Oak Ridge, TN 37831-0062
www.osti.gov
Phone: (865) 576-8401
Fax: (865) 576-5728
Email: reports@osti.gov

Disclaimer

This report was prepared as an account of work sponsored by an agency of the United States Government. Neither the United States Government nor any agency thereof, nor UChicago Argonne, LLC, nor any of their employees or officers, makes any warranty, express or implied, or assumes any legal liability or responsibility for the accuracy, completeness, or usefulness of any information, apparatus, product, or process disclosed, or represents that its use would not infringe privately owned rights. Reference herein to any specific commercial product, process, or service by trade name, trademark, manufacturer, or otherwise, does not necessarily constitute or imply its endorsement, recommendation, or favoring by the United States Government or any agency thereof. The views and opinions of document authors expressed herein do not necessarily state or reflect those of the United States Government or any agency thereof, Argonne National Laboratory, or UChicago Argonne, LLC.

A model of annular linear induction pump

prepared by
Yoichi Momozaki
Nuclear Engineering Division, Argonne National Laboratory

10/27/2016

Table of Contents

Part-I: Electro-Magneto-Dynamic part	1
Defining traveling current waves	4
Relating the applied current to the distributed coil system and the applied traveling current wave	6
Magnetic flux in the core and magnetic field strength in the gap.....	7
Relating the magnetic field and magnetic flux with the traveling current wave using a magnetic circuit model	8
Calculating the induced current waves.....	10
Induced current in the working fluid	10
Induced current in the duct walls and other components	11
Determining unknowns.....	11
Calculating the developed pressure per pole	14
Calculating the power input per pole	15
Comparing with R. Rüdénberg’s and R. S. Baker’s work.....	16
References	20
Part-II: Electrical part	21
Equivalent circuit	22
Phasor	23
Calculating the values for various electrical parameters.....	24
Coil wiring configuration.....	28
References	30
Part-III Transport effects (End effects).....	31
Modeling the ALIP in 1-D	31
Solving the differential equation	34
Infinitely long pump case.....	38
References	40
Part-IV Calculation procedures	41
Design calculation procedure	41
Input parameters	41

Calculating various major parameters	42
Determining the duct and air gap dimensions.....	42
Determining the fluid dynamic pressure loss	43
Determining the actual applied voltage	43
Performance calculation procedure	47
Input parameters	47
Calculating various major parameters	47
Calculate the duct and air gap dimensions	48
Calculate the stator dimensions	48
Calculate the coil parameters	48
Calculate the fluid dynamic pressure loss.....	48
Calculate some parameters	49
Calculating the overall pump size	50
Calculating the overall pump efficiency.....	50
Calculating the end effect	50

A model of annular linear induction pumps

Yoichi Momozaki

Part-I: Electro-Magneto-Dynamic part

To model an annular linear induction pump, we assume a pump within which a periodic, traveling electrical current wave along the axis of the pump exists (Figure 1 and Figure 2). This is same as to treat the pump as an infinitely long pump.

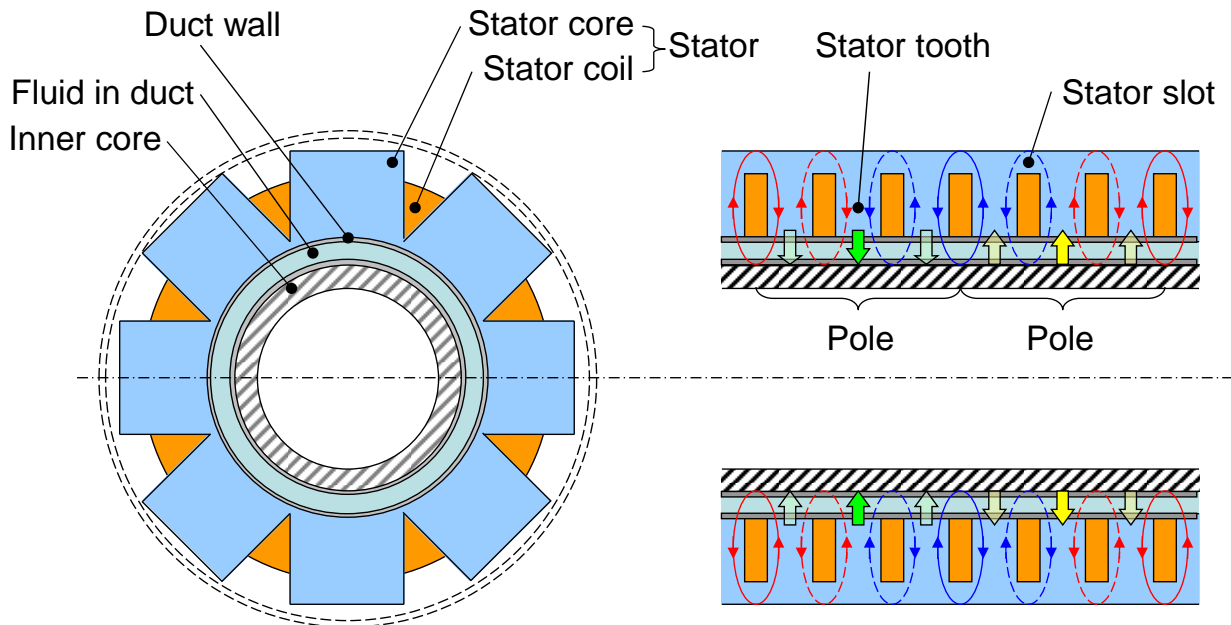


Figure 1. Schematic of an annular linear induction pump.

The traveling current wave flowing in the azimuthal direction, I_{θ} (pink line shown in Figure 3) produces a traveling magnetic flux in the core, Φ_c (blue line in Figure 3) from Ampere's law. Note that the current itself flows in the azimuthal direction, however the wave travels along the axial direction. An associated traveling magnetic field in the pump duct, $B_{\perp ra}$ (green line in Figure 3) follows the traveling magnetic flux in the core from Gauss's law for magnetism. The magnetic field in the pump duct is in the radial direction, but the wave is traveling along the axial direction. This traveling magnetic flux in the core, Φ_c also induces an induction current wave around the center core, $I_{\theta ind}$ from Faraday's law of induction. Resulting Lorentz force thrusts the electrically conductive fluid in the pump. The traveling current wave is the sum of an externally applied periodic, traveling current sheet (or wave), $I_{\theta ap}$ (orange line in Figure 3)

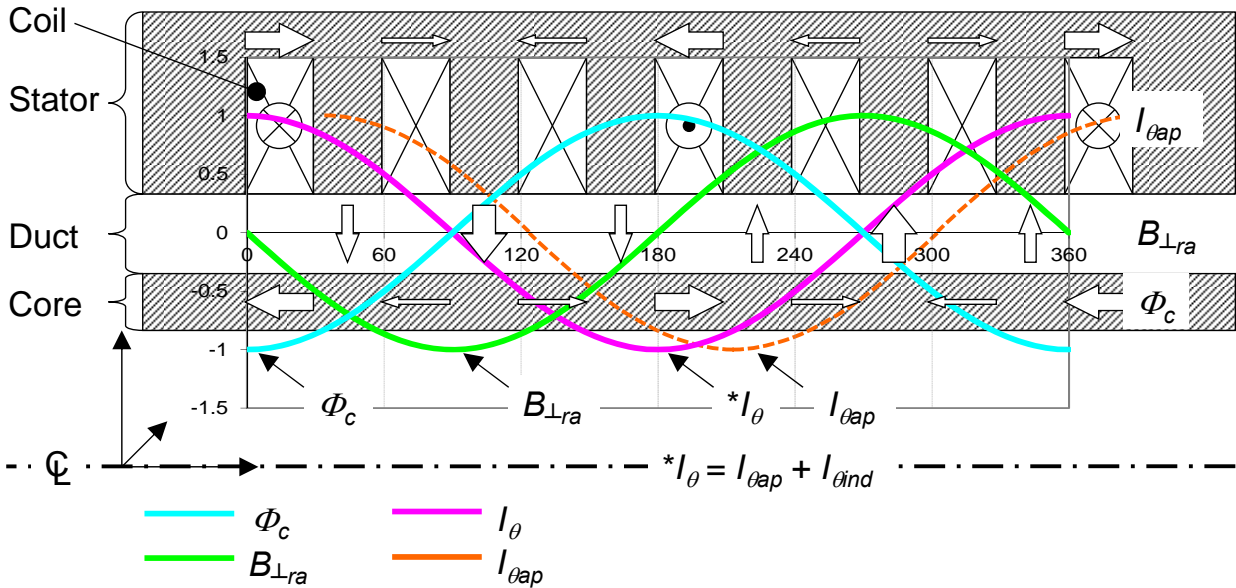


Figure 3. Schematic of various traveling waves in the pump.

Typical coil connection with 3 phase power supply

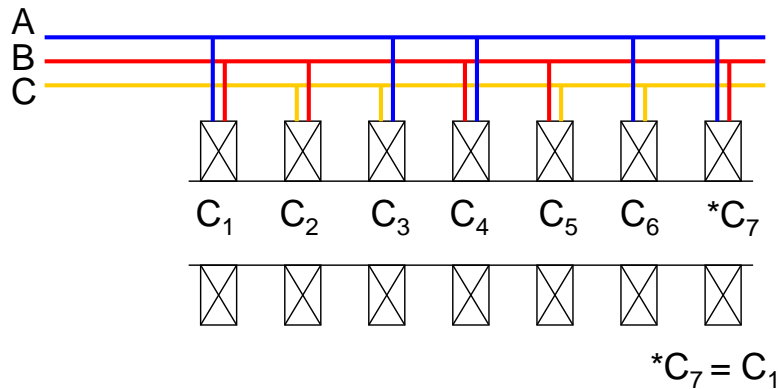


Figure 4. Schematic of distributed coils and their connections to 3 phase power supply.

Using this method, various parameters per each wavelength (or 2 x poles) of the waves may be calculated and by adding the thrust per pole up to the total number of the poles in the pump, the total pump pressure head developed by the pump with a finite length may be approximated without solving a complex system of temporal-spatial differential equations.

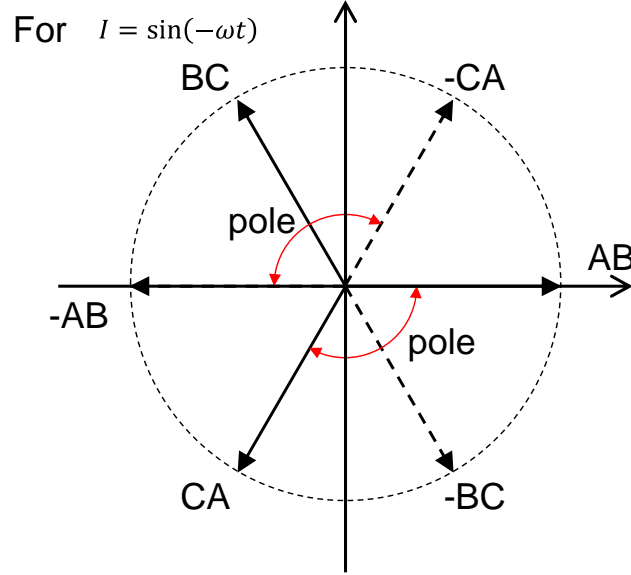


Figure 5. Phase relationship of the coil connection with 3 phase power.

The present work explains how the magnetic field and the induced current are obtained when the distributed coils are powered by a 3 phase power supply. From the magnetic field and the induced current, the thrust and the induction losses in the pump can be calculated to estimate the pump performance.

Defining traveling current waves

The applied traveling current wave may be expressed as:

$$I'_{\theta ap}(t, z) = I'_{\theta appk} \exp i(-\omega t + kz), \quad [1]$$

where $I'_{\theta appk}$ is the peak value of the linear density of the applied traveling current wave, $\omega = 2\pi f_{dr} = \frac{2\pi}{2l_{pp}} v_s$, $k = \frac{2\pi}{2l_{pp}}$, where l_{pp} is the pole pitch ($l_{pp} = \frac{L_p}{N_{pole}}$ where L_p is the pump length, N_{pole} is the number of poles), v_s is the synchronous velocity of the current wave. We used $\exp i(\theta) = \cos\theta + i\sin\theta$ where i is the imaginary unit. Note that the current is flowing in the azimuthal direction (θ direction) in the coils surrounding the core and the wave is traveling along the pump (z direction).

Knowing that the induced current is periodic, the linear current density, $I'_{\theta ind}(t, z)$ induced in the working fluid may be assumed as:

$$I'_{\theta ind}(t, z) = I'_{\theta indpk} \exp i(-\omega t + kz + \phi), \quad [2]$$

where $I'_{\theta indpk}$ is the peak value of the induced linear current density and ϕ is the phase difference between the applied current and the induced current. Note that the current is flowing in the azimuthal direction (θ direction) in the pump annular duct and the wave is

traveling along the pump (z direction). Also note that $I'_{\theta\text{indpk}}$ and ϕ are unknown constants and are to be determined. In addition to $I'_{\theta\text{ind}}$, there are induction currents in the duct walls and other components where the changing magnetic field exists. These induction currents, which do not flow in the working fluid and do not contribute for pumping, may be expressed as:

$$\Delta I'_{\theta\text{ind}}(t, z) = \Delta I'_{\theta\text{indpk}} \exp i(-\omega t + kz + \phi), \quad [3]$$

The total traveling current wave in the pump, $I'_{\theta\text{tot}}(t, z)$ is the sum of the induced current wave and the applied current wave so that:

$$I'_{\theta\text{tot}}(t, z) = I'_{\theta\text{ind}}(t, z) + \Delta I'_{\theta\text{ind}}(t, z) + I'_{\theta\text{ap}}(t, z), \quad [4]$$

which can be rewritten as:

$$I'_{\theta\text{tot}}(t, z) = I'_{\theta\text{appk}} [\beta(1 + \Delta_w) \exp i(-\omega t + kz + \phi) + \exp i(-\omega t + kz)], \quad [5]$$

where $\beta = \frac{I'_{\theta\text{indpk}}}{I'_{\theta\text{appk}}}$ and $\Delta_w = \frac{\Delta I'_{\theta\text{indpk}}}{I'_{\theta\text{indpk}}}$, which are unknowns due to $I'_{\theta\text{indpk}}$ and $\Delta I'_{\theta\text{indpk}}$. Note that using β , the $I'_{\theta\text{ind}}$ and $\Delta I'_{\theta\text{ind}}$ may be expressed in terms of $I'_{\theta\text{appk}}$ as:

$$I'_{\theta\text{ind}}(t, z) = I'_{\theta\text{appk}} \beta \exp i(-\omega t + kz + \phi), \quad [6]$$

and

$$I'_{\theta\text{ind}}(t, z) + \Delta I'_{\theta\text{ind}}(t, z) = I'_{\theta\text{appk}} \beta_c \exp i(-\omega t + kz + \phi), \quad [7]$$

where $\beta_c = \beta(1 + \Delta_w)$. The total traveling current wave (eq. [5]) can be further calculated as:

$$\begin{aligned} I'_{\theta\text{tot}}(t, z) &= I'_{\theta\text{appk}} [\beta_c \cos \phi + 1 + \beta_c i \sin \phi] \exp i(-\omega t + kz) \\ &= I'_{\theta\text{appk}} \sqrt{(\beta_c \cos \phi + 1)^2 + (\beta_c \sin \phi)^2} \exp i(-\omega t + kz + \psi), \end{aligned} \quad [8]$$

where:

$$\psi = \arctan \left(\frac{\beta_c \sin \phi}{\beta_c \cos \phi + 1} \right), \quad [9]$$

and $I'_{\theta\text{totpk}}$ is now defined as:

$$I'_{\theta\text{totpk}} = I'_{\theta\text{appk}} \sqrt{(\beta_c \cos \phi + 1)^2 + (\beta_c \sin \phi)^2}, \quad [10]$$

so that:

$$I'_{\theta\text{tot}}(t, z) = I'_{\theta\text{totpk}} \exp i(-\omega t + kz + \psi). \quad [11]$$

Relating the applied current to the distributed coil system and the applied traveling current wave

Note in a real ALIP, the magnetomotive force due to the total applied current per pole, $I_{\theta\text{aptp}}p$ is $\sin(\theta) + \sin\left(\theta + \frac{1}{3}\pi\right) + \sin\left(\theta + \frac{2}{3}\pi\right)$ for $0 \leq \theta \leq \frac{1}{3}\pi$ times the total current flowing through the coil that is the peak current, $I_{\theta\text{appk}}$ times the number of turns, N_{turns} times the number of coils per phase per pole, N_{pppp} (see Figure 6). By taking average, $I_{\theta\text{aptp}}p$ may be expressed as:

$$\begin{aligned} I_{\theta\text{aptp}}p &= I_{\theta\text{appk}} \int_0^{\frac{1}{3}\pi} \left[\sin(\theta) + \sin\left(\theta + \frac{1}{3}\pi\right) + \sin\left(\theta + \frac{2}{3}\pi\right) \right] d\theta / \left(\frac{1}{3}\pi\right) \\ &\quad \times N_{\text{turns}} \times N_{\text{pppp}} \\ &= \frac{6}{\pi} I_{\theta\text{appk}} \times N_{\text{turns}} \times N_{\text{pppp}}. \end{aligned} \quad [12]$$

Also the magnetomotive force due to the applied traveling current wave per pole is calculated as:

$$I_{\theta\text{aptp}}p = \int_0^{l_{pp}} I'_{\theta\text{ap}} dz = \frac{2l_{pp}}{\pi} I'_{\theta\text{appk}}. \quad [13]$$

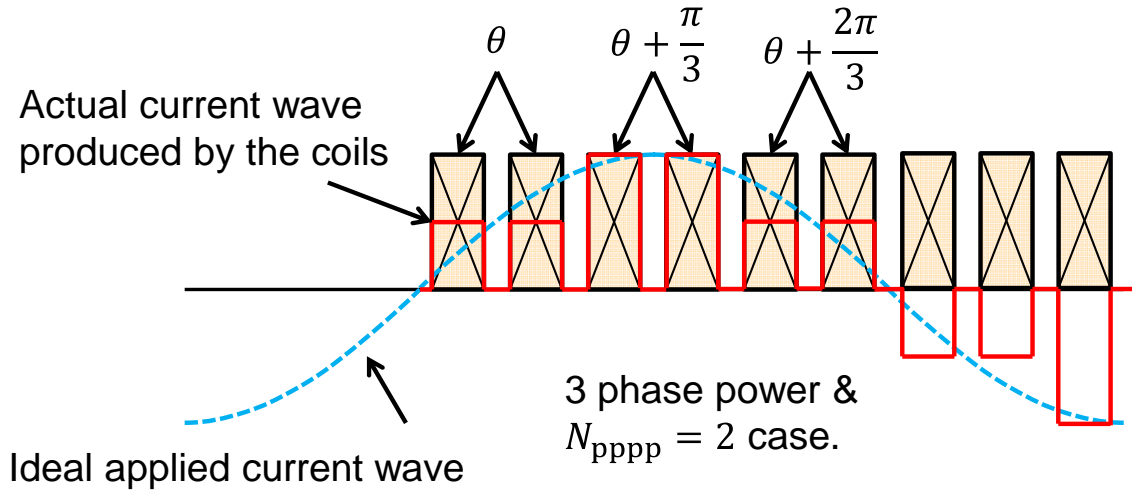


Figure 6. Relationship of the current wave and the applied current wave produced by the distributed coil system.

By equating above 2 equations, the peak applied current density to the coil, $I'_{\theta\text{appk}}$ can be calculated from the peak applied current to the coil, $I_{\theta\text{appk}}$ as:

$$I'_{\theta\text{appk}} = \frac{3N_{\text{turns}}N_{\text{pppp}}}{l_{pp}} I_{\theta\text{appk}}. \quad [14]$$

In fact above conversion (actual current to linear current density) is valid for all traveling current waves.

Also the magnetomotive force due to the total traveling current wave per pole is calculated as:

$$I_{\theta\text{totpp}} = \int_0^{l_{pp}} I'_{\theta\text{tot}} dz = \frac{2l_{pp}}{\pi} I'_{\theta\text{totpk}}. \quad [15]$$

Magnetic flux in the core and magnetic field strength in the gap

The magnetic flux in the center core, Φ_c is in the same phase with $I'_{\theta\text{tot}}$ as to think of coils wrapping around the core. The magnetic flux in the core may be expressed as:

$$\Phi_c = \Phi_{\text{cpk}} \exp(-\omega t + kz + \psi), \quad [16]$$

Note that from the continuity of the magnetic flux,

$$B_{ra} = -\frac{1}{l_{\text{aave}}} \frac{\partial \Phi_c}{\partial z}, \quad [17]$$

where l_{aave} is the average circumference of the air gap (center line of the flow path annulus), see Figure 7.

$$\begin{aligned} B_{ra} &= -\frac{1}{l_{\text{aave}}} \Phi_{\text{cpk}} k i \exp(-\omega t + kz + \psi) \\ &= \frac{1}{l_{\text{aave}}} \Phi_{\text{cpk}} k \exp\left(-\omega t + kz + \psi + \frac{\pi}{2} + \pi\right), \end{aligned} \quad [18]$$

where we used $i \exp(i\theta) = \exp\left(\theta + \frac{\pi}{2}\right)$ and $-\exp(i\theta) = \exp(\theta + \pi)$.

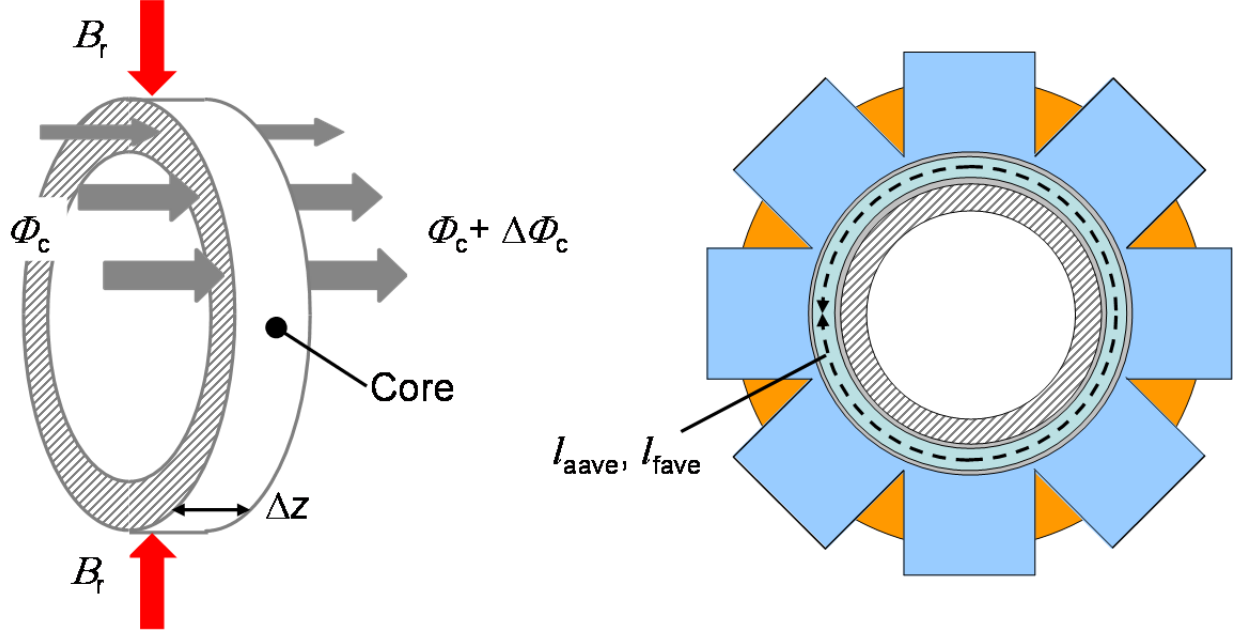


Figure 7. Relationship between the magnetic flux in the core and radial magnetic field strength.

The peak value of the magnetic field strength, B_{rapk} , may be defined as:

$$B_{ra} = B_{rapk} \exp i \left(-\omega t + kz + \psi + \frac{\pi}{2} + \pi \right), \quad [19]$$

where:

$$B_{rapk} = \frac{1}{l_{aave}} \frac{\pi}{l_{pp}} \Phi_{cpk}, \text{ or} \quad [20]$$

$$\Phi_{cpk} = \frac{1}{\pi} B_{rapk} \cdot l_{aave} \cdot l_{pp}. \quad [21]$$

Relating the magnetic field and magnetic flux with the traveling current wave using a magnetic circuit model

We consider an infinitesimal magnetic circuit shown in Figure 8. We assume μ in iron core is that $\mu \gg \mu_0$ such that the magnetic reluctance in the iron structures (stator core and center core) is neglected. The magnetic reluctance in the air gap may be expressed as, see Figure 8:

$$dR = 1 / \left(\frac{\mu_0 \cdot l_{aave} dz}{\tau_a \cdot C_{c2}} \right), \quad [22]$$

where Carter coefficient, C_{c2} is used to include the effects of slot structures in the stator cores. The radial magnetic flux is obtained as:

$$\Phi_p(z) = B_{ra}(z) l_{aave} dz. \quad [23]$$

The magnetomotive force is:

$$\text{mmf}(z) = I'_{\theta\text{tot}}(t, z)dz. \quad [24]$$

Following change of the magnetomotive force occurs along the magnetic circuit from 1 to 4 (Figure 8):

$$0 + \Phi_p \left(z - \frac{1}{2} dz \right) dR + \text{mmf}(z) - \Phi_p \left(z + \frac{1}{2} dz \right) dR = 0. \quad [25]$$

By substituting each term in the above equation, the equation becomes:

$$\frac{d}{dz} \left[B_{\text{rapk}} \exp i \left(-\omega t + kz + \psi + \frac{\pi}{2} + \pi \right) \right] dz \frac{\tau_a \cdot C_{c2}}{\mu_0} = I'_{\theta\text{totpk}} \exp i (-\omega t + kz + \psi) dz, \quad [26]$$

then:

$$k B_{\text{rapk}} \exp i (-\omega t + kz + \psi) \frac{\tau_a \cdot C_{c2}}{\mu_0} = I'_{\theta\text{totpk}} \exp i (-\omega t + kz + \psi), \quad [27]$$

and finally,

$$I'_{\theta\text{totpk}} = B_{\text{rapk}} \frac{\pi \tau_a \cdot C_{c2}}{\mu_0 \cdot l_{\text{pp}} l_{\text{aave}}} l_{\text{aave}} = B_{\text{rapk}} \mathcal{R}_{ma} l_{\text{aave}}. \quad [28]$$

where:

$$\mathcal{R}_{ma} = \frac{\pi \tau_a \cdot C_{c2}}{\mu_0 \cdot l_{\text{pp}} l_{\text{aave}}}, \quad [29]$$

is the magnetic reluctance of the air gap.

Now both B_{rapk} and Φ_{cpk} can be expressed in terms of $I'_{\theta\text{totpk}}$ as:

$$B_{\text{rapk}} = \frac{1}{\mathcal{R}_{ma} l_{\text{aave}}} I'_{\theta\text{totpk}}, \quad [30]$$

$$\Phi_{\text{cpk}} = \frac{1}{\mathcal{R}_{ma}} \frac{l_{\text{pp}}}{\pi} I'_{\theta\text{totpk}}. \quad [31]$$

$$I'_{\theta\text{ind}} = \frac{\tau_f \sigma_f}{l_{\text{fave}}} k \Delta v i \Phi_c. \quad [35]$$

Substituting Φ_c from eq. [16] yields:

$$I'_{\theta\text{ind}} = \frac{\tau_f \sigma_f}{l_{\text{fave}}} k \Delta v \Phi_{\text{cpk}} i \exp(-\omega t + kz + \psi), \quad [36]$$

and with eq. [21]:

$$I'_{\theta\text{ind}} = \frac{\tau_f \sigma_f l_{\text{aave}}}{l_{\text{fave}}} \Delta v B_{\text{rapk}} \exp\left(-\omega t + kz + \psi + \frac{\pi}{2}\right). \quad [37]$$

Induced current in the duct walls and other components

The induced current in the duct walls, $\Delta I'_{\theta\text{ind}}$ may be expressed as (similar step as eq. [34] and eq. [35]):

$$\Delta I'_{\theta\text{ind}} = -\frac{\tau_w \sigma_w}{l_{\text{wave}}} \frac{\partial \Phi_c}{\partial t}, \quad [38]$$

where the subscript “w” denotes the values for the duct walls. There may be more components in the air gap where the induced current exist. The contributions from these components may be summed and represented by the duct walls. Note that since the walls do not have relative movement to the pump, regular temporal derivative instead of material derivative is taken. Performing temporal derivative gives:

$$\begin{aligned} \Delta I'_{\theta\text{ind}} &= \frac{\tau_w \sigma_w}{l_{\text{wave}}} k v_s i \Phi_c \\ &= w_i I'_{\theta\text{ind}}, \end{aligned} \quad [39]$$

where $w_i = \frac{\tau_w \sigma_w}{\tau_f \sigma_f} \frac{l_{\text{fave}}}{l_{\text{wave}}} \frac{v_s}{\Delta v}$, so that:

$$I'_{\theta\text{ind}} + \Delta I'_{\theta\text{ind}} = (1 + w_i) \frac{\tau_f \sigma_f l_{\text{aave}}}{l_{\text{fave}}} \Delta v B_{\text{rapk}} \exp\left(-\omega t + kz + \psi + \frac{\pi}{2}\right). \quad [40]$$

Determining unknowns

Substitute eq. [7] and B_{rapk} from eq. [30] into eq. [40]:

$$\begin{aligned} &I'_{\theta\text{appk}} \beta_c \exp(-\omega t + kz + \phi) \\ &= (1 + w_i) \frac{\tau_f \sigma_f}{l_{\text{fave}}} \frac{1}{\mathcal{R}_{\text{ma}}} \frac{l_{\text{pp}}}{\pi} k \Delta v I'_{\theta\text{totpk}} \exp\left(-\omega t + kz + \psi + \frac{\pi}{2}\right). \end{aligned} \quad [41]$$

Substituting $I'_{\theta\text{totpk}}$ from eq. [10] yields:

$$\begin{aligned} &I'_{\theta\text{appk}} \beta_c \exp(-\omega t + kz + \phi) \\ &= (1 + w_i) \frac{\tau_f \sigma_f}{l_{\text{fave}}} \frac{1}{\mathcal{R}_{\text{ma}}} \frac{l_{\text{pp}}}{\pi} k \Delta v I'_{\theta\text{appk}} \sqrt{(\beta_c \cos \phi + 1)^2 + (\beta_c \sin \phi)^2} \\ &\quad \times \exp\left(-\omega t + kz + \psi + \frac{\pi}{2}\right). \end{aligned} \quad [42]$$

Comparing LHS and RHS of above equation and substituting $\psi = \arctan\left(\frac{\beta_c \sin\phi}{\beta_c \cos\phi + 1}\right)$ from eq. [9], following relationships can be obtained from the equation above:

$$\beta_c = (1 + w_i) \frac{\tau_f \sigma_f}{l_{fave}} \frac{1}{\mathcal{R}_{ma}} \frac{l_{pp}}{\pi} k \Delta v \sqrt{(\beta_c \cos\phi + 1)^2 + (\beta_c \sin\phi)^2}, \quad [43]$$

$$\psi = \phi - \frac{\pi}{2}, \text{ and} \quad [44]$$

$$\frac{\beta_c \sin\phi}{\beta_c \cos\phi + 1} = \tan\left(\phi - \frac{\pi}{2}\right). \quad [45]$$

Calculating $\tan\left(\phi - \frac{\pi}{2}\right)$ above gives the following relationship:

$$\beta_c [(\sin\phi)^2 + (\cos\phi)^2] = \beta_c = -\cos\phi. \quad [46]$$

Substituting $\cos\phi = -\beta_c$ into eq. [43] gives:

$$\beta_c = (1 + w_i) \frac{\tau_f \sigma_f}{l_{fave}} \frac{1}{\mathcal{R}_{ma}} \frac{l_{pp}}{\pi} k \Delta v \sqrt{1 - \beta_c^2}, \quad [47]$$

which can be solved for β_c while noting that RHS of eq. [43] is positive so that:

$$\beta_c = \frac{\alpha}{\sqrt{1 + \alpha^2}}, \quad [48]$$

where

$$\alpha = (1 + w_i) \frac{\tau_f \sigma_f}{l_{fave}} \frac{1}{\mathcal{R}_{ma}} \Delta v. \quad [49]$$

With $\beta_c = -\cos\phi$, it follows that:

$$\sin\phi = \pm \sqrt{1 - \beta_c^2}, \quad [50]$$

and because of the relationship between $I'_{\theta ind} + \Delta I'_{\theta ind}$ and $I'_{\theta tot}$, we take the positive sign, see Figure 9.

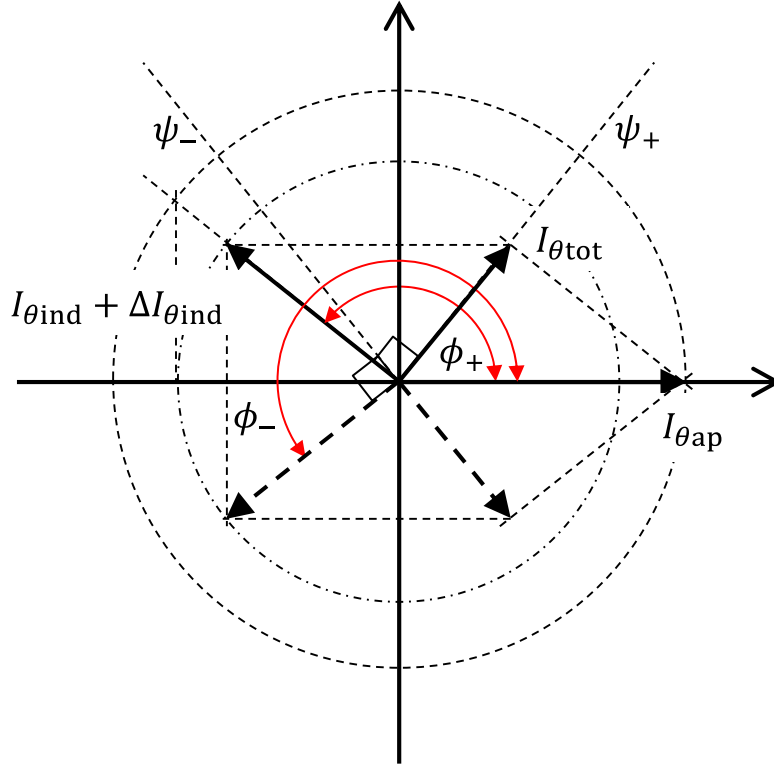


Figure 9. Schematic showing the relationship between the applied, induced, and total currents for the positive sign case and the negative sign case. When negative is taken ($I_{\theta\text{ind}} + \Delta I_{\theta\text{ind}}$ in the 3rd quadrant at ϕ_- indicated by a dashed arrow), the total current, $I_{\theta\text{tot}}$ (indicated by another dashed arrow, the sum of $I_{\theta\text{ind}} + \Delta I_{\theta\text{ind}}$ and $I_{\theta\text{ap}}$) is in the 4th quadrant whereas ψ_- is in the 2nd quadrant from eq. [44], becoming out of 180° .

Therefore:

$$\tan\phi = -\frac{\sqrt{1-\beta_c^2}}{\beta_c} = -\frac{1}{\alpha}. \quad [51]$$

Then it follows that:

$$\phi = -\arctan\left(\frac{1}{\alpha}\right), \quad [52]$$

where $\frac{\pi}{2} \leq \phi \leq \pi$.

As a summary, now we can calculate the magnetic field strength in the annular gap (eq. [19]) and the induced current in the working fluid (eq. [37]) from the applied current as:

$$B_{\text{ra}} = B_{\text{rapk}} \exp\left(-\omega t + kz - \arctan\left(\frac{1}{\alpha}\right) + \pi\right), \quad [53]$$

$$I'_{\theta\text{ind}} = \frac{\tau_f \sigma_f l_{\text{aave}}}{l_{\text{fave}}} \Delta v B_{\text{rapk}} \exp\left(-\omega t + kz - \arctan\left(\frac{1}{\alpha}\right)\right). \quad [54]$$

where (from eq. [30], eq. [10], and eq. [48]):

$$B_{\text{rapk}} = \frac{1}{\mathcal{R}_{\text{ma}} l_{\text{aave}}} \frac{1}{\sqrt{1+\alpha^2}} I'_{\theta\text{appk}}, \text{ and} \quad [55]$$

$$\alpha = (1 + w_i) \frac{\tau_f \sigma_f}{l_{\text{fave}}} \frac{1}{\mathcal{R}_{\text{ma}}} \Delta v. \quad [56]$$

Also note that from eq. [6], eq. [54], and eq. [55]:

$$\beta = \frac{\tau_f \sigma_f}{l_{\text{fave}}} \Delta v \frac{1}{\mathcal{R}_{\text{ma}}} \frac{1}{\sqrt{1+\alpha^2}}, \quad [57]$$

and substituting eq. [48] and eq. [49] above gives:

$$\beta = \frac{1}{1+w_i} \beta_c, \quad [58]$$

Therefore by definition:

$$\Delta_w = w_i. \quad [59]$$

Calculating the developed pressure per pole

The developed pressure due to Lorentz force is given as:

$$\frac{dP}{dz} = \mathbf{j}_{\text{ind}} \times \mathbf{B}. \quad [60]$$

Note the direction of the force in the pump ($\frac{dP}{dz} < 0$ gives positive pumping, see Figure 2). The induced current density in the working fluid, $J_{\theta\text{ind}}$ can be calculated from $I'_{\theta\text{ind}}$ (eq. [54]) as:

$$J_{\theta\text{ind}} = \frac{\sigma_f l_{\text{aave}}}{l_{\text{fave}}} \Delta v B_{\text{rapk}} \text{expi}(-\omega t + kz + \phi). \quad [61]$$

The magnetic field strength that the working fluid experiences may be assumed the same as the magnetic field strength in the gap that is (from eq. [19], note the phase and the sign):

$$B_{\text{ra}} = -B_{\text{rapk}} \text{expi}(-\omega t + kz + \phi). \quad [62]$$

Note that the negative sign appearing in eq. [62] makes the pumping positive and physically consistent. The induced current density in the working fluid is in the azimuthal direction and the magnetic field is in the radial direction so that they are perpendicular to each other.

Replacing $\text{expi}(-\omega t + kz + \phi)$ with $\cos(-\omega t + kz + \phi)$ for the real notation, the developed pressure per pole can be calculated as:

$$\Delta P_{\text{pp}} = \int_{-\frac{1}{2}l_{\text{pp}}}^{\frac{1}{2}l_{\text{pp}}} \frac{dP}{dz} dz$$

$$\begin{aligned}
&= \sigma_f \frac{l_{aave}}{l_{fave}} \Delta v B_{rapk}^2 \int_{-\frac{1}{2}l_{pp}}^{\frac{1}{2}l_{pp}} [\cos(-\omega t + kz + \phi)]^2 dz \\
&= \frac{1}{2} l_{pp} \sigma_f \frac{l_{aave}}{l_{fave}} \Delta v B_{rapk}^2.
\end{aligned} \tag{63}$$

Substituting eq. [55] above gives:

$$\Delta P_{pp} = \frac{1}{2} l_{pp} \sigma_f \frac{l_{aave}}{l_{fave}} \Delta v \left(\frac{1}{\mathcal{R}_{ma} l_{aave}} \right)^2 \frac{1}{1+\alpha^2} I'_{\theta appk}{}^2, \tag{64}$$

where $\alpha = (1 + w_i) \frac{\tau_f \sigma_f}{l_{fave} \mathcal{R}_{ma}} \Delta v$.

Calculating the power input per pole

The total power input to the working fluid per pole, W_{fpp} is the sum of the thermal power and the kinetic power due to the induction. The thermal power input is actually Joule heating and volumetric Joule heating, w'''_{fh} is given as:

$$w'''_{fh} = \frac{J_{\theta ind}^2}{\sigma_f}. \tag{65}$$

The volumetric kinetic power, w'''_{fKE} is given as:

$$w'''_{fKE} = \frac{dP}{dz} v_f. \tag{66}$$

The volumetric total power input is:

$$w'''_f = \frac{J_{\theta ind}^2}{\sigma_f} + \frac{dP}{dz} v_f = \frac{J_{\theta ind}^2}{\sigma_f} + J_{\theta ind} B_{ra} v_f. \tag{67}$$

Substituting eq. [61] and eq. [62] into the above equation gives:

$$\begin{aligned}
w'''_f &= \sigma_f \Delta v^2 \left(\frac{l_{aave}}{l_{fave}} \right)^2 B_{ra}^2 + \sigma_f \Delta v \left(\frac{l_{aave}}{l_{fave}} \right) B_{ra}^2 v_f \\
&= \sigma_f \Delta v B_{ra}^2 \left(\frac{l_{aave}}{l_{fave}} \right) \left[\left(\frac{l_{aave}}{l_{fave}} \right) v_s + \frac{l_{fave} - l_{aave}}{l_{fave}} v_f \right],
\end{aligned} \tag{68}$$

and noting that $\frac{l_{aave}}{l_{fave}} \cong 1$ so that $\frac{l_{fave} - l_{aave}}{l_{fave}} \cong 0$, which gives:

$$w'''_f \cong \sigma_f \Delta v B_{ra}^2 \left(\frac{l_{aave}}{l_{fave}} \right)^2 v_s, \tag{69}$$

that is:

$$w'''_f \cong \left(\frac{l_{aave}}{l_{fave}} \right) \frac{dP}{dz} v_s \cong \frac{dP}{dz} v_s. \tag{70}$$

meaning that the total power input to the working fluid is the product of the pressure and the synchronous velocity (whereas the pumping power is the product of the pressure and the fluid velocity). Also note that:

$$w'''_f \cong \sigma_f \Delta v^2 B_{ra}^2 \frac{v_s}{\Delta v} = \frac{J_{\theta ind}^2}{\sigma_f} \frac{1}{s}, \quad [71]$$

where $s = \frac{\Delta v}{v_s}$ that is slip, meaning that the effective load of the working fluid can be viewed as an electrical resistive load of $\frac{R_f}{s}$ where R_f is the actual resistive load of the working fluid calculated from the properties of the fluid and the geometry of the annular duct that contains the fluid.

The total power input to the working fluid per pole is then given as:

$$W_{fpp} \cong \Delta P_{pp} Q \frac{v_s}{v_f}, \quad [72]$$

or from eq. [69]:

$$W_{fpp} \cong \frac{1}{2} l_{pp} \sigma_f \left(\frac{l_{aave}}{l_{fave}} \right)^2 \Delta v B_{rapk}^2 \tau_f l_{fave} v_s. \quad [73]$$

Since the pump components that experience the changing magnetic field (in this work, represented by the duct walls) are not moving with the working fluid, by following the similar steps described above, the power input to the duct walls per pole, W_{wpp} may be given as:

$$W_{wpp} \cong \frac{1}{2} l_{pp} \sigma_w \left(\frac{l_{aave}}{l_{wave}} \right)^2 v_s B_{rapk}^2 \tau_w l_{wave} v_s. \quad [74]$$

This corresponds to the power input to the duct walls due to $\Delta I'_{\theta ind}$. With $w_i = \frac{\tau_w \sigma_w l_{fave} v_s}{\tau_f \sigma_f l_{wave} \Delta v}$, the sum of the induction losses is therefore given as:

$$W_{fpp} + W_{wpp} \cong (1 + w_i) \frac{1}{2} l_{pp} \sigma_f \left(\frac{l_{aave}}{l_{fave}} \right)^2 \Delta v B_{rapk}^2 \tau_f l_{fave} v_s = (1 + w_i) W_{fpp}. \quad [75]$$

Comparing with R. Rüdénberg's and R. S. Baker's work

Baker derived a similar expression for a flat linear induction pump (FLIP), Ref. [1], based on Rüdénberg's prior work (Ref. [2]). The total force produced by the pump, F given by Eq. [91] in Baker's work with notations used in our work becomes:

$$F = \frac{1}{4} \tau \sigma_f \Delta v B_m^2 \lambda^2 N_{pole} \left(\frac{\left(\frac{l_{pp} + \lambda}{\lambda} \right)}{(4\mu\lambda\Delta v\sigma_f)^2 + \left(\frac{l_{pp} + \lambda}{\lambda} \right)^2} \right), \quad [76]$$

where τ is the duct height and λ is the width of the duct since this is for the FLIP with a duct with a rectangular cross section. The resistivity of the working fluid is replaced with the

reciprocal of the conductivity of the working fluid. B_m is the peak magnetic field produced only by the applied current. We believe that Baker's eqs. [90] and [91] contain an error such that $4\mu\lambda$ is missing in the denominator of the RHS. For the zero fluid velocity case, the equivalent equations are given as eq. [70] and eq. [71] in Baker's work, which correctly contain $4\mu\lambda$ (or l that is $4\mu\lambda$, see eq. [46] in his work). Or check eq. [27] on pg. 297 of the prior work by Rüdénberg (Ref [2]), which is the same equation as eq. [70] of Baker's.

By dividing by the duct cross sectional area, $\lambda\tau$ and removing the number of poles from the equation above, the developed pressure per pole is expressed as:

$$\Delta P_{pp} = \frac{1}{4}\sigma_f\Delta v B_m^2 \lambda \left(\frac{\left(\frac{l_{pp} + \lambda}{\lambda} + \frac{\lambda}{l_{pp}}\right)}{(4\mu\lambda\Delta v\sigma_f)^2 + \left(\frac{l_{pp} + \lambda}{\lambda} + \frac{\lambda}{l_{pp}}\right)^2} \right). \quad [77]$$

Note that Baker's work was performed using CGS (Gaussian units system). Converting this equation in SI unit system ($4\pi\mu \rightarrow \mu_0$) gives:

$$\Delta P_{pp} = \frac{1}{4}\sigma_f\Delta v B_m^2 \lambda \left(\frac{\left(\frac{l_{pp} + \lambda}{\lambda} + \frac{\lambda}{l_{pp}}\right)}{\left(\frac{\mu_0}{\pi}\lambda\Delta v\sigma_f\right)^2 + \left(\frac{l_{pp} + \lambda}{\lambda} + \frac{\lambda}{l_{pp}}\right)^2} \right), \quad [78]$$

or rewriting the above equation respect to B_m^2 ,

$$B_m^2 = \frac{2\Delta P_{pp}}{\sigma_f l_{pp} \Delta v} \left(\frac{2 \left[\left(\frac{\mu_0}{\pi}\lambda\Delta v\sigma_f\right)^2 + \left(\frac{l_{pp} + \lambda}{\lambda} + \frac{\lambda}{l_{pp}}\right)^2 \right]}{1 + \left(\frac{\lambda}{l_{pp}}\right)^2} \right), \quad [79]$$

which is Rüdénberg equation (Ref. [3]). Note that in Ref. [3], to use Rüdénberg equation in an ALIP, the width of the duct, λ for a rectangular duct had been replaced with the equivalent duct width for an annular duct, $\frac{A_a}{\tau_a}$ where A_a is the cross sectional area of the annular duct. We will show it later, but this replacement to adapt Rüdénberg equation to the ALIP configuration is not sufficient. Rearranging eq. [78] yields:

$$\Delta P_{pp} = \frac{1}{4}\sigma_f\Delta v B_m^2 \lambda \frac{l_{pp}}{\lambda} \left(\frac{\left(\left(\frac{l_{pp}}{\lambda}\right)^2 + 1\right)}{\left(\frac{\mu_0}{\pi}\Delta v\sigma_f l_{pp}\right)^2 + \left(\left(\frac{l_{pp}}{\lambda}\right)^2 + 1\right)^2} \right). \quad [80]$$

Now we adapt the above equation to an ALIP geometry. Note that the FLIP has a rectangular duct and it has a cosine distribution over the width of the duct, whereas an ALIP has an annular duct that has no ends in its circumference direction so that it has a uniform distribution along the circumference direction. In Baker's work on pg. 20, between eq. [67] and

eq. [68], it was shown that the cosine distribution resulted in $\frac{1}{2}\lambda$ factor in the equation above, whereas for the ALIP case with same width of the duct (width of the FLIP = circumference of the ALIP) it should be:

$$\int_{-\frac{\lambda}{2}}^{\frac{\lambda}{2}} 1 dy = \lambda, \quad [81]$$

so the factor $\frac{1}{2}\lambda$ in eq. [80] is replaced with λ that yields:

$$\Delta P_{pp} = \frac{1}{2} l_{pp} \sigma_f \Delta v B_m^2 \left(\frac{\left(\left(\frac{l_{pp}}{\lambda} \right)^2 + 1 \right)}{\left(\frac{\mu_0 \Delta v \sigma_f l_{pp}}{\pi} \right)^2 + \left(\left(\frac{l_{pp}}{\lambda} \right)^2 + 1 \right)^2} \right). \quad [82]$$

Also for the ALIP geometry, $\frac{l_{pp}}{\lambda} \rightarrow 0$ since the duct has no ends in the circumference direction, which gives:

$$\begin{aligned} \Delta P_{pp} &= \lim_{\frac{l_{pp}}{\lambda} \rightarrow 0} \frac{1}{2} l_{pp} \sigma_f \Delta v B_m^2 \left(\frac{\left(\left(\frac{l_{pp}}{\lambda} \right)^2 + 1 \right)}{\left(\frac{\mu_0 \Delta v \sigma_f l_{pp}}{\pi} \right)^2 + \left(\left(\frac{l_{pp}}{\lambda} \right)^2 + 1 \right)^2} \right) \\ &= \frac{1}{2} l_{pp} \sigma_f \Delta v B_m^2 \left(\frac{1}{1 + \left(\frac{\mu_0 \Delta v \sigma_f l_{pp}}{\pi} \right)^2} \right). \end{aligned} \quad [83]$$

Using the relationship given by eq. [30] of the present work, B_m may be expressed with the peak applied linear current density, $I'_{\theta appk}$ in the same way as:

$$B_m = \frac{1}{\mathcal{R}_{ma} l_{aave}} I'_{\theta appk}, \quad [84]$$

so that:

$$\Delta P_{pp} = \frac{1}{2} l_{pp} \sigma_f \Delta v \left(\frac{1}{\mathcal{R}_{ma} l_{aave}} \right)^2 \left(\frac{1}{1 + \left(\frac{\mu_0 \Delta v \sigma_f l_{pp}}{\pi} \right)^2} \right) I'_{\theta appk}{}^2. \quad [85]$$

The above expression is the equivalent of eq. [64] of the present work but derived from Baker's works. Eq. [64] of the present work is expressed as:

$$\Delta P_{pp} = \frac{1}{2} l_{pp} \sigma_f \Delta v \left(\frac{1}{\mathcal{R}_{ma} l_{aave}} \right)^2 \left(\frac{l_{aave}}{l_{fave}} \right) \left(\frac{1}{1 + \left[(1+w_i) \frac{\tau_f l_{aave}}{\tau_a l_{fave}} \cdot \frac{1}{c_{c2}} \cdot \frac{\mu_0 \Delta v \sigma_f l_{pp}}{\pi} \right]^2} \right) I'_{\theta appk}{}^2. \quad [86]$$

By comparing eq. [85] and eq. [86], it is clear that the present work includes the effects due to the difference between the air gap dimensions and the dimensions of the gap that is occupied by the fluid. Also the effects of the slots in the stator cores to the air gap are included by Carter coefficient, C_{c2} . The effect of the induction losses in the duct is also included by w_i . Baker's expression appears to assume that the air gap dimensions and the dimensions of the gap that is occupied by the fluid are the same. Also it will not be able to include the effects of the slots in the stator cores and the induction losses in the duct walls, but otherwise the expression is the same as the present work, which further strengthen the validity of the current work.

References

1. R. S. Baker, (1956) "Calculation of developed pressure and fluid power in linear polyphaser induction liquid metal pumps," Technical Report 48, Mine Safety Appliances company, Callery, PA.
2. R. Rüdberg, (1907) "Energie der Wirbelströme in elektrischen Bremsen und Dynamomaschinen," Sammlung elektrotechnischer Vorträge, pp 269-370.
3. J. B. Colson, G. W. Olsen, (1971) "FEFPL: Annular Linear Induction Pump Configuration Comparisons," FEFPL-ALIP Sm-74-71, Interoffice correspondence, Idaho Nuclear Corporation.

Part-II: Electrical part

We assume a pump within which a periodic, traveling electrical current wave along the axis of the pump exists. In the part-I of the present work, the EMD aspect of the model was discussed. Although the model requires 3 phase alternating current as a major input parameter, normally a 3 phase system provides prescribed 3 phase voltage (Figure 1). For a delta connected ALIP, it is typically the line-to-line voltage. To obtain the required 3 phase current from the prescribed 3 phase voltage source, an electrical circuit analysis is needed, which is described in this part-II of the present work.

Typical coil connection with 3 phase power supply

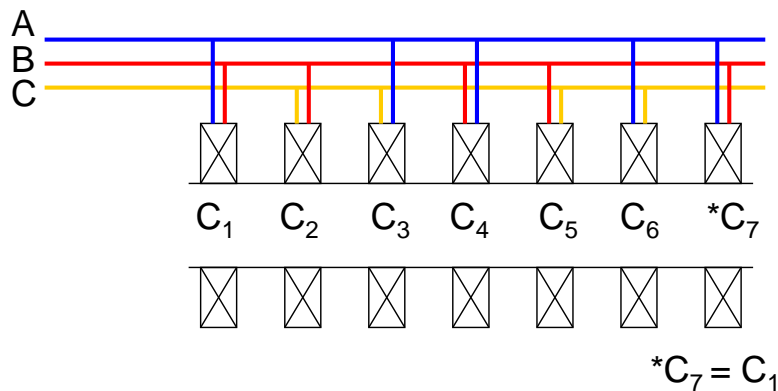


Figure 1. Schematic of distributed coils and their connections to 3 phase power supply.

The part-II of the present work explains how the applied current and voltage to the coil system in the pump is obtained when the distributed coils are powered by a 3 phase power supply. Using the calculated applied current and the voltage, the pump parameters can be calculated with the part-I of the present work.

Equivalent circuit

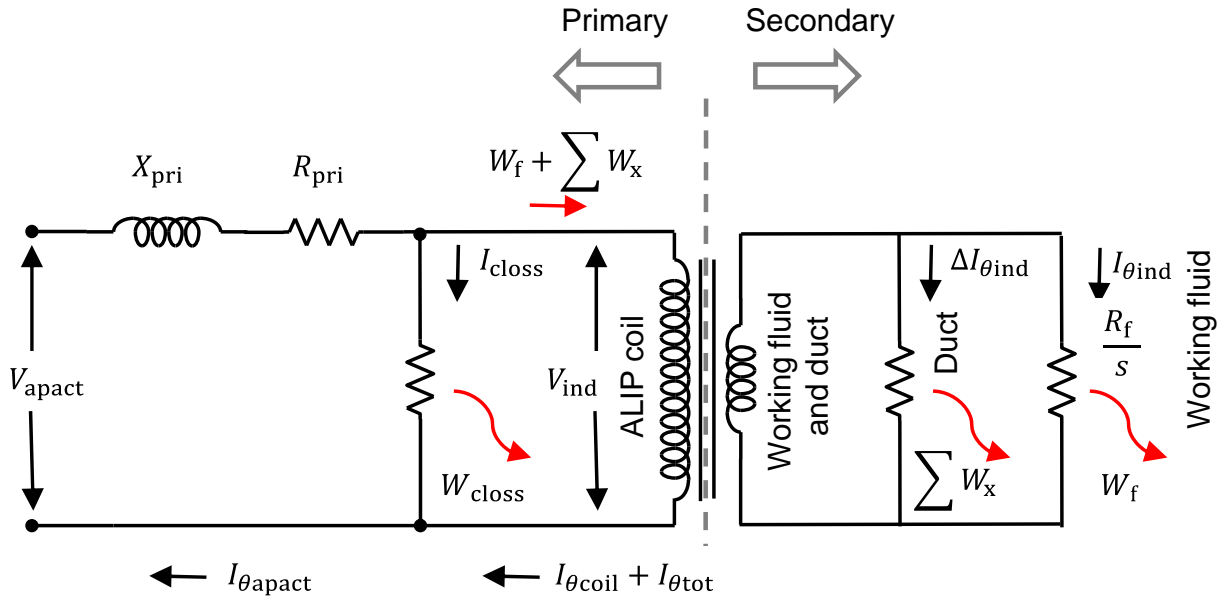


Figure 2. Schematic of an equivalent electrical circuit of ALIP and the red arrows indicate flow of power.

An equivalent circuit for an ALIP is developed and is schematically shown in Figure 2. The coils in the pump surround the center core as a primary coil and the working fluid in the annular duct as well as the duct itself also surround the center core as a secondary one-turn coil. This may be viewed as a transformer. The applied voltage to a coil is V_{apact} and the induced voltage across the coil is V_{ind} . The coil has reactance, X_{pri} due to the leakage flux in the coil (the magnetic flux generated by the coils that does not link with the working fluid and duct walls) and resistance, R_{pri} , for example see Ref. [4]. These values are calculated from the coil properties and the coil configuration. The coil requires primary current, $I_{\theta coil}$ to supply $I_{\theta ind} + \Delta I_{\theta ind}$ to the secondary (the working fluid and the duct) in addition to current for the core losses, I_{closs} . I_{closs} corresponds to the power dissipated in the core and other structures, W_{closs} . $I_{\theta tot}$ is the magnetizing current. In the secondary, $I_{\theta ind}$ corresponds to the power input to the working fluid, W_f and $\Delta I_{\theta ind}$ corresponds to the power dissipated in the duct walls, $\sum W_x$. Because the working fluid and the duct completely surround the center core, we assume that there is negligible leakage flux in the secondary side (the working fluid and the duct), which is equivalent of having a pure resistive load on the secondary.

Phasor

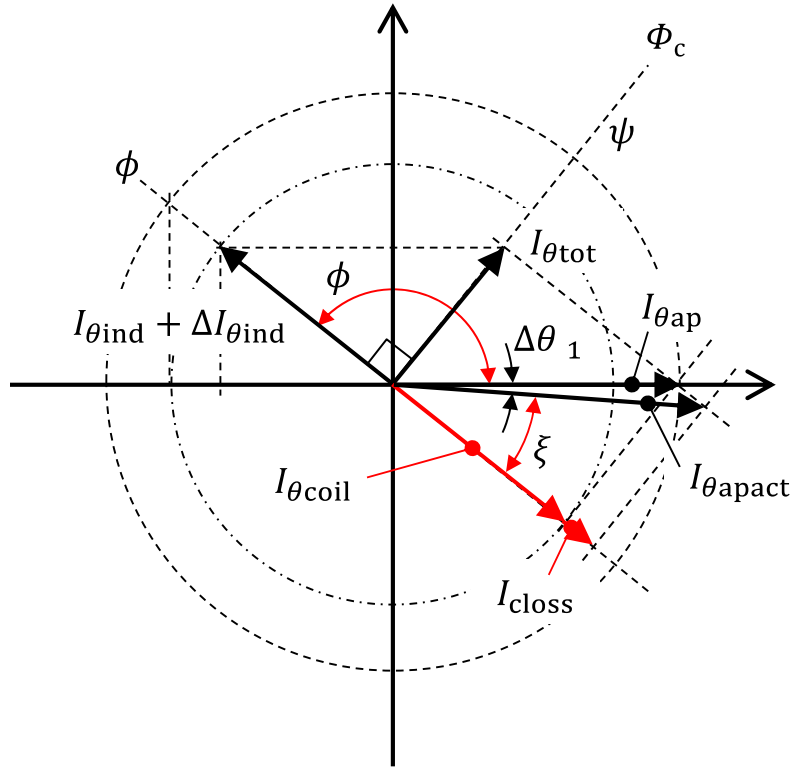


Figure 3. Phasor indicating various currents.

From the part-I of the present work (Figure 9 of the part-I), a phasor is drawn in Figure 3. Since there is no reactance in the secondary, the secondary current ($= I_{\theta ind} + \Delta I_{\theta ind}$) is exactly 90° behind the core flux, Φ_c at ψ . Note that the current waves are moving at $\exp i(-\omega t + kz)$ and in this schematic, the clockwise direction is the direction of the rotation. In the part-I, the relationship between $I_{\theta ind} + \Delta I_{\theta ind}$, $I_{\theta tot}$, and $I_{\theta ap}$ was derived assuming no core losses. However in a real ALIP, there are some core losses and the primary (coil) needs to provide additional current shown as I_{closs} . The actual coil current, $I_{\theta apact}$ is the vector sum of $I_{\theta ap}$ and I_{closs} . The current in the primary side to supply $I_{\theta ind} + \Delta I_{\theta ind}$ is I_{coil} .

Figure 4 shows the voltage relationship in another phasor. The induced EMF in the coil is V_{ind} that is at 90° to the core flux, Φ_c . There are additional voltage drops in the coil associated with X_{pri} and R_{pri} . They are proportional to the actual coil current, $I_{\theta apact}$ while $I_{\theta apact} X_{pri}$ is at 90° to $I_{\theta apact}$ and $I_{\theta apact} R_{pri}$ is in phase with $I_{\theta apact}$ by definition.

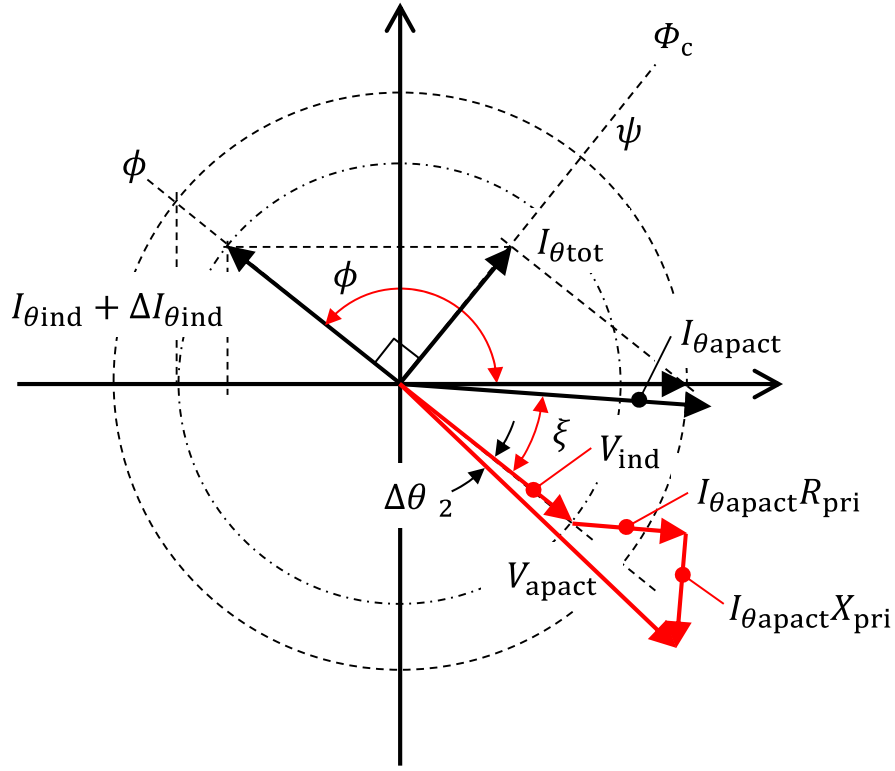


Figure 4. Phasor indicating various voltages.

Calculating the values for various electrical parameters

From eq. [72] of the part-I of the present work, the power to the working fluid per pole is given as:

$$W_{fpp} = \Delta P_{pp} Q \frac{v_s}{v_f}, \quad [1]$$

or eq. [73] of the part-I:

$$W_{fpp} \cong \frac{1}{2} l_{pp} \sigma_f \left(\frac{l_{aave}}{l_{fave}} \right)^2 \Delta v B_{rapk}^2 \tau_f l_{fave} v_s. \quad [2]$$

Also using eq. [75] of the part-I, the power to the various components per pole is:

$$\begin{aligned} W_{fpp} + \sum_x W_{xpp} &\cong W_{fpp} + W_{wpp} = (1 + w_i) W_{fpp} \\ &= (1 + w_i) \frac{1}{2} l_{pp} \sigma_f \left(\frac{l_{aave}}{l_{fave}} \right)^2 \Delta v B_{rapk}^2 \tau_f l_{fave} v_s. \end{aligned} \quad [3]$$

We assume such that the core loss per pole, $W_{closspp}$ needs to be separately specified as an input.

There are $6 \times N_{pppp}$ coils that are needed to complete a cycle, which consists of 2 poles. Each pole contains $3 \times N_{pppp}$ coils. Therefore the amount of power each coil needs to deliver can be calculated from the various power per pole as:

$$W_{\text{coil}} = \frac{W_{\text{closspp}} + W_{\text{fpp}} + \sum_x W_{\text{xpp}}}{3N_{pppp}}. \quad [4]$$

For an AC system, the electrical input, W is given as $W = \frac{1}{2} V_{\text{pk}} I_{\text{pk}}$ where V_{pk} is the peak value of the applied voltage and I_{pk} is the peak value of the current in phase with the voltage. The amount of the current in phase with the voltage, V_{ind} that the coil needs may be divided into two parts as $I_{\theta\text{coil}}$ and I_{closs} , see Figure 3 so that:

$$I_{\theta\text{coilpk}} = \frac{W_{\text{fpp}} + \sum_x W_{\text{xpp}}}{3N_{pppp} \times \frac{1}{2} V_{\text{indpk}}}, \text{ and} \quad [5]$$

$$I_{\text{closspk}} = \frac{W_{\text{closspp}}}{3N_{pppp} \times \frac{1}{2} V_{\text{indpk}}}, \quad [6]$$

where:

$$V_{\text{ind}} = - \left(-N_{\text{turns}} \frac{d\phi_c}{dt} \right) = -N_{\text{turns}} \omega \Phi_{\text{cpk}} \exp i \left(-\omega t + kz + \psi + \frac{\pi}{2} \right), \quad [7]$$

so that:

$$V_{\text{indpk}} = N_{\text{turns}} \omega \Phi_{\text{cpk}}, \quad [8]$$

from Lenz's law. Note that the minus sign in eq. [7] for V_{ind} is to counteract against the EMF induced by Lenz's law. Note that eq. [6] may also be written as:

$$I_{\theta\text{coilpk}} = \frac{(1+w_i) \frac{1}{2} l_{\text{pp}} \sigma_f \left(\frac{l_{\text{aave}}}{l_{\text{fave}}} \right)^2 \Delta v B_{\text{rapk}}^2 \tau_f l_{\text{fave}} v_s}{3N_{pppp} \times \frac{1}{2} V_{\text{indpk}}}, \quad [9]$$

and substituting eq. [20] of the part-I yields:

$$I_{\theta\text{coilpk}} = \frac{\frac{l_{\text{pp}}}{\pi} (1+w_i) l_{\text{pp}} \sigma_f \left(\frac{l_{\text{aave}}}{l_{\text{fave}}} \right)^2 \Delta v \left(\frac{\pi}{l_{\text{aave}} \cdot l_{\text{pp}}} \right)^2 \Phi_{\text{cpk}} \tau_f l_{\text{fave}}}{3 \times N_{\text{turns}} \times N_{pppp}}. \quad [10]$$

From eq. [14] with eq. [28], both from the part-I, $I_{\theta\text{totpk}}$ maybe obtained as:

$$I_{\theta\text{totpk}} = \frac{B_{\text{rapk}} \mathcal{R}_{\text{ma}} l_{\text{aave}} l_{\text{pp}}}{3 \times N_{\text{turns}} \times N_{pppp}}, \quad [11]$$

or using eq. [20] of the part-I, the above expression can be rewritten with Φ_{cpk} as:

$$I_{\theta\text{totpk}} = \frac{\pi \Phi_{\text{cpk}} \mathcal{R}_{\text{ma}}}{3 \times N_{\text{turns}} \times N_{pppp}}. \quad [12]$$

Note that $I_{\theta_{\text{coilpk}}}$ may be expressed as:

$$I_{\theta_{\text{coilpk}}} = \frac{\frac{l_{\text{pp}}}{\pi}(1+w_i)l_{\text{pp}}\sigma_f\left(\frac{l_{\text{aave}}}{l_{\text{fave}}}\right)^2 \Delta v \left(\frac{\pi}{l_{\text{aave}} \cdot l_{\text{pp}}}\right)^2 \Phi_{\text{cpk}} \tau_f l_{\text{fave}}}{\pi \Phi_{\text{cpk}} \mathcal{R}_{\text{ma}}} I_{\theta_{\text{totpk}}} \\ = \alpha I_{\theta_{\text{totpk}}}, \quad [13]$$

where α is from eq. [49] of the part-I.

The angle between $I_{\theta_{\text{tot}}}$ and $I_{\theta_{\text{ap}}}$ is ψ or $\phi - \frac{\pi}{2}$ so the angle between $I_{\theta_{\text{ap}}}$ and $I_{\theta_{\text{coil}}}$ is $\psi - \frac{\pi}{2}$. The angle between $I_{\theta_{\text{apact}}}$ and $I_{\theta_{\text{coil}}}$ is given as $\xi = \psi - \frac{\pi}{2} - \Delta\theta_1$ (note that with this definition, $\xi < 0$ and $\Delta\theta_1 < 0$). Therefore the following relationship can be established (see Figure 3):

$$\xi = -\tan\left(\frac{I_{\theta_{\text{totpk}}}}{I_{\theta_{\text{coilpk}}} + I_{\text{closspk}}}\right), \quad [14]$$

and:

$$\Delta\theta_1 = \xi - \psi + \frac{\pi}{2}, \quad [15]$$

and also:

$$I_{\theta_{\text{apactpk}}} = \sqrt{(I_{\theta_{\text{coilpk}}} + I_{\text{closspk}})^2 + I_{\theta_{\text{totpk}}}^2}. \quad [16]$$

Finally:

$$I_{\theta_{\text{apact}}} = I_{\theta_{\text{apactpk}}} \exp i(-\omega t + kz + \Delta\theta_1). \quad [17]$$

From Figure 4 and Figure 5, it follows that:

$$V_{\theta_{\text{apactpk}}} = \sqrt{(V_{\text{indpk}} \cos \xi + I_{\theta_{\text{apactpk}}} R_{\text{pri}})^2 + (V_{\text{indpk}} \sin \xi - I_{\theta_{\text{apactpk}}} X_{\text{pri}})^2}. \quad [18]$$

Note that $V_{\text{indpk}} \sin \xi < 0$. Also

$$\tan(\xi + \Delta\theta_2) = \frac{V_{\text{indpk}} \sin \xi - I_{\theta_{\text{apactpk}}} X_{\text{pri}}}{V_{\text{indpk}} \cos \xi + I_{\theta_{\text{apactpk}}} R_{\text{pri}}}, \quad [19]$$

(note that with this definition, $\Delta\theta_2 < 0$) so that:

$$\Delta\theta_2 = \arctan\left(\frac{V_{\text{indpk}} \sin \xi - I_{\theta_{\text{apactpk}}} X_{\text{pri}}}{V_{\text{indpk}} \cos \xi + I_{\theta_{\text{apactpk}}} R_{\text{pri}}}\right) - \xi. \quad [20]$$

Finally:

$$V_{\theta_{\text{apact}}} = V_{\theta_{\text{apactpk}}} \exp i(-\omega t + kz + \Delta\theta_1 + \xi + \Delta\theta_2). \quad [21]$$

The real power input per coil is:

$$P_{\text{coilre}} = \frac{1}{2} V_{\theta_{\text{apactpk}}} I_{\theta_{\text{apactpk}}} \cos(\xi + \Delta\theta_2). \quad [22]$$

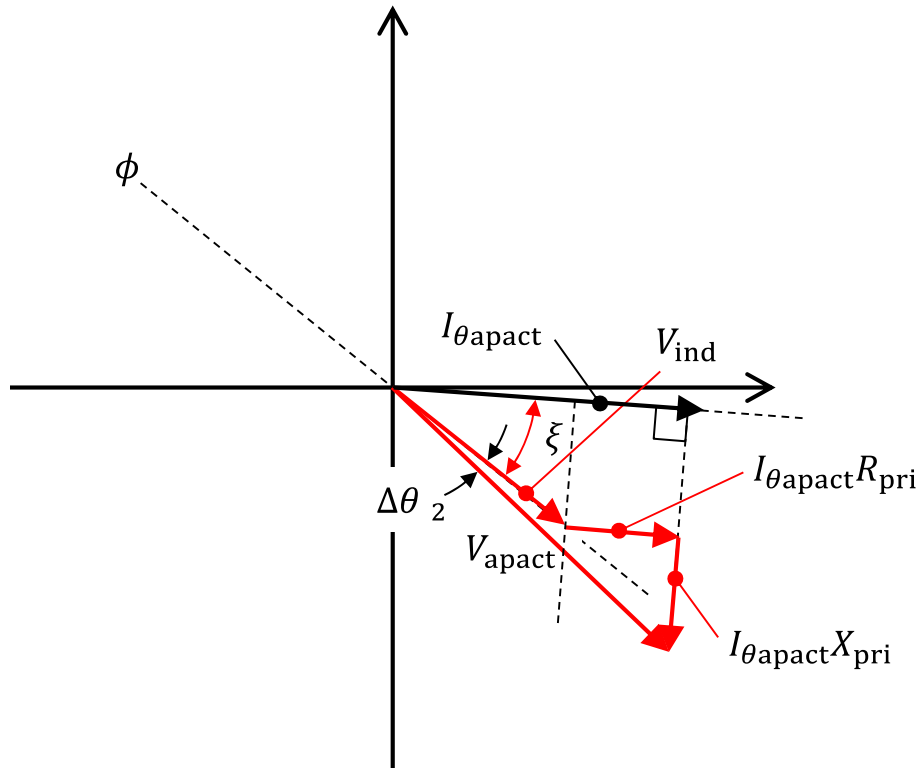


Figure 5. Relationship between V_{ind} and $V_{\theta_{\text{apact}}}$.

Now we know the voltage, $V_{\theta_{\text{apact}}}$ and the current, $I_{\theta_{\text{apact}}}$ that each coil needs to be provided and the line-to-line voltage and the phase and the line currents can be calculated depending on how the coils are wired together.

Coil wiring configuration

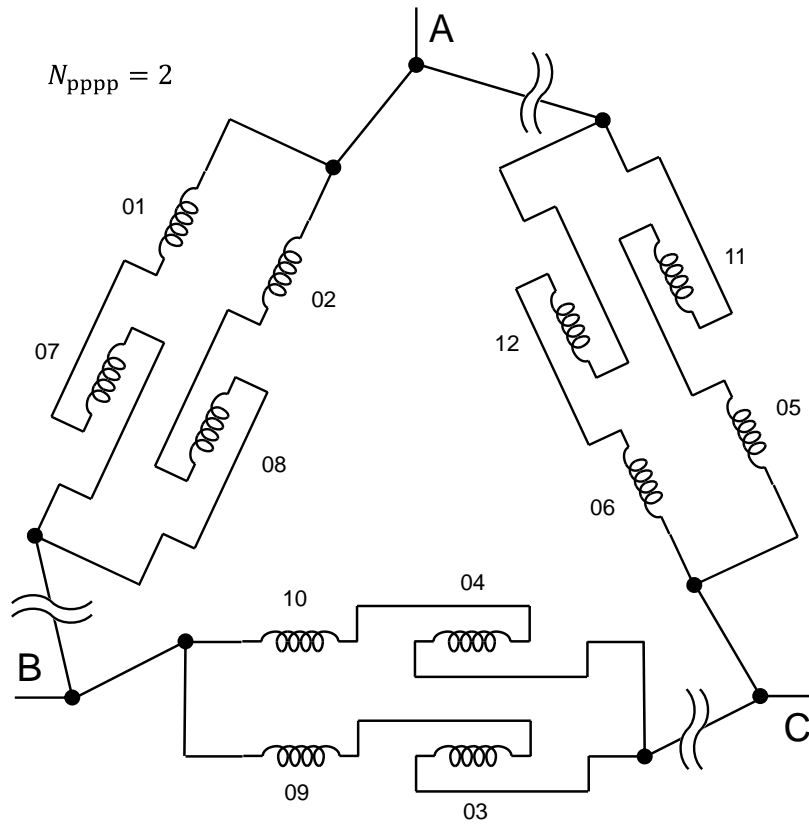


Figure 6. An example of coil wiring diagram.

Each coil can be wired in any way as long as its relative phase relationship to the other coils is correctly maintained. In this section, we consider a typical wiring scheme as an example, see Figure 6. The figure shows a typical case with a 3 phase power supply. For a complete cycle (2 poles), the required number of coils is $6 \times N_{pppp}$. In this example, $N_{pppp} = 2$ and the coils that are in the same pole and the same phase (that are also physically next to each other) are in parallel (for example, coils #1 and #2). But the coils that are in the different phases are connected in series (for example, coils #1 and #3). Each group of coils between 2 phases per cycle contains $2 \times N_{pppp}$ coils or 4 coils in this example. 2 coils (one in the first pole and another in the second pole) are connected in series and N_{pppp} coils are in parallel. The groups of the $2 \times N_{pppp}$ coils are connected in series. The number of groups between 2 phases is $\frac{N_{poles}}{2}$. The final line-to-line voltage is:

$$V_{LL} = 2 \times \frac{N_{poles}}{2} V_{\theta_{apact}} = N_{poles} V_{\theta_{apact}}, \quad [23]$$

and the phase current is:

$$I_p = N_{pppp} I_{\theta \text{apact}}.$$

[24]

References

4. A. S. Langsdorf, (1955) *Theory of alternating-current machinery*, McGraw-Hill.

Part-III Transport effects (End effects)

In the part-III of the present work, a simple 1-D model (pump axial dimension) of an ALIP is developed and the end effect is analytically calculated based on the work described in the part-I and part-II.

Modeling the ALIP in 1-D

In this model, an $r - \theta - z$ coordinate is employed. The pump axis is set as the z axis (Figure 1). The varying applied current, $I_{\theta ap}(t, z)$ is applied to the coils surrounding the annular duct and the core. The length of the pump is L_p so that there are 2 boundaries, one at $z = -\frac{1}{2}L_p$ and another at $z = \frac{1}{2}L_p$. The applied current is assumed to have only θ component. In the core, an axial magnetic flux, $\Phi_c(t, z)$ is produced by the applied current (and resulting induced current). The magnetic flux is assumed to have only z component. The magnetic flux in the core then induces the induced current, $I_{\theta ind}(t, z)$ in the working fluid in the annular duct. The induced current is also assumed to have only θ component. Because of the spatial variation of the magnetic flux in the core, the radial magnetic field strength, $B_{ra}(t, z)$ exists in the annular duct region. Although the radial magnetic field changes with r , assuming the thickness of the annular duct is small compared with the ID or OD of the duct, we may assume that $B_{ra}(t, z)$ is only a function of time and axial location.

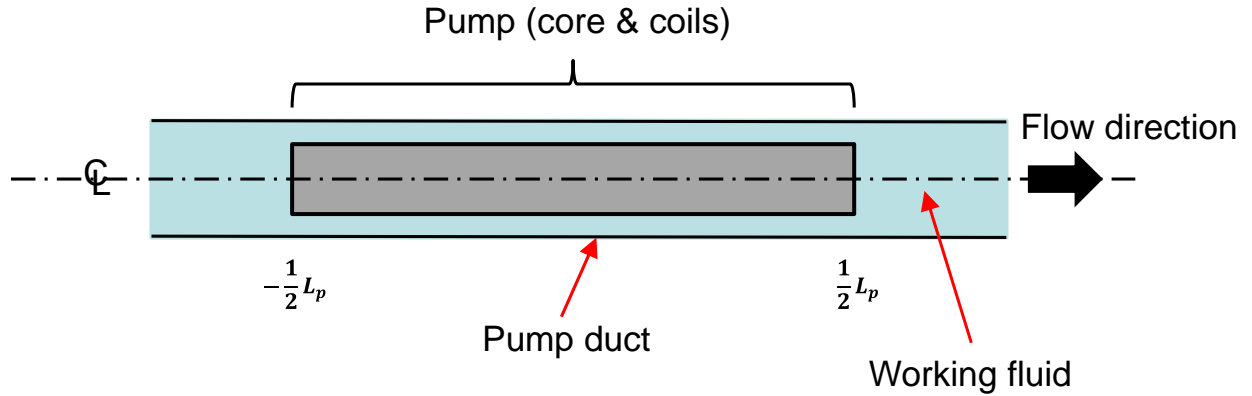


Figure 1. Schematic of the pump model.

The applied traveling current wave may be expressed as, see eq. [1] of part-I:

$$I'_{\theta ap}(t, z) = I'_{\theta appk} \exp i(-\omega t + kz). \quad [1]$$

The total traveling current wave in the pump, $I'_{\theta tot}(t, z)$ is the sum of the induced current waves and the applied current wave, see eq. [4] of part-I:

$$I'_{\theta\text{tot}}(t, z) = I'_{\theta\text{ind}}(t, z) + \Delta I'_{\theta\text{ind}}(t, z) + I'_{\theta\text{ap}}(t, z), \quad [2]$$

From the continuity of the magnetic flux (see eq. [17] of the part-I),

$$B_{ra} = -\frac{1}{l_{\text{aave}}} \frac{\partial \Phi_c}{\partial z}, \quad [3]$$

where l_{aave} is the average circumference of the air gap. From Ampere's law:

$$\sum_k \mu_k J_{\theta k} = \mu_x J_{\theta\text{tot}} = \frac{\partial B_{ra}}{\partial z}. \quad [4]$$

Since there are several different components (represented by k, for example, in this work we assumed that the annular air gap consists of the following 3 components: air gap, working fluid, and the duct walls) in the annular air gap, the overall effect from the circumferential current flowing in each component may be added as shown in the above equation. In the equation above, μ_k is the permeability of and $J_{\theta k}$ is the circumferential current density in each component. Also an infinitesimal current in the air gap flowing in the circumferential direction is expressed as $dI_{\theta k} = I'_{\theta k} dz = J_{\theta k} \tau_k dz$ where τ_k is the thickness of the component in the air gap, which are assumed constant over the pump. By introducing a subscript x to represent the summed quantity of all the components in the gap, the equation above can be rewritten as:

$$I'_{\theta\text{tot}} = \frac{\tau_x}{\mu_x} \frac{\partial B_{ra}}{\partial z}. \quad [5]$$

We will discuss how to set μ_x and τ_x later. Substituting eq.[2] and eq. [3] into eq. [5] gives:

$$-\frac{\tau_x}{\mu_x l_{\text{aave}}} \frac{\partial^2 \Phi_c}{\partial z^2} = I'_{\theta\text{ind}} + \Delta I'_{\theta\text{ind}} + I'_{\theta\text{ap}}. \quad [6]$$

Also from eq. [34] and eq. [39] of the part-I, the induced current waves can be expressed as:

$$I'_{\theta\text{ind}} + \Delta I'_{\theta\text{ind}} = -(1 + w_i) \frac{\tau_f \sigma_f}{l_{\text{fave}}} \left(\frac{\partial}{\partial t} + v_f \frac{\partial}{\partial z} \right) \Phi_c. \quad [7]$$

Substituting eq. [7] into eq. [6] gives:

$$-\frac{\tau_x}{\mu_x l_{\text{aave}}} \frac{\partial^2 \Phi_c}{\partial z^2} = -(1 + w_i) \frac{\tau_f \sigma_f}{l_{\text{fave}}} \left(\frac{\partial}{\partial t} + v_f \frac{\partial}{\partial z} \right) \Phi_c + I'_{\theta\text{ap}}, \quad [8]$$

where: $w_i = \frac{\tau_w \sigma_w}{\tau_f \sigma_f} \frac{l_{\text{fave}}}{l_{\text{wave}}} \frac{v_s}{\Delta v}$ (see the part-I).

Also from Figure 3 of the part-II:

$$I_{\theta\text{ap}} = I_{\theta\text{coil}} + I_{\theta\text{tot}}. \quad [9]$$

With eq. [14] of the part-I, the applied current may be converted to the linear current density of the applied current as:

$$I'_{\theta ap} = \frac{3N_{\text{turns}}N_{\text{pppp}}}{l_{\text{pp}}} (I_{\theta \text{coil}} + I_{\theta \text{tot}}), \quad [10]$$

and substituting eq. [10] and eq. [12] both from the part-II into the above equation gives:

$$I'_{\theta ap} = \frac{1}{l_{\text{pp}}} \times \left(\frac{l_{\text{pp}}}{\pi} (1 + w_i) l_{\text{pp}} \sigma_f \left(\frac{l_{\text{aave}}}{l_{\text{fave}}} \right)^2 \Delta v \left(\frac{\pi}{l_{\text{aave}} l_{\text{pp}}} \right)^2 \Phi_{\text{cpk}} \tau_f l_{\text{fave}} \exp i \left(-\omega t + kz + \psi - \frac{\pi}{2} \right) + \pi \Phi_{\text{cpk}} \mathcal{R}_{\text{ma}} \exp i (-\omega t + kz + \psi) \right). \quad [11]$$

Introducing:

$$\Gamma = \frac{1}{l_{\text{pp}}} \times \left[\left(\frac{l_{\text{pp}}}{\pi} (1 + w_i) l_{\text{pp}} \sigma_f \left(\frac{l_{\text{aave}}}{l_{\text{fave}}} \right)^2 \Delta v \left(\frac{\pi}{l_{\text{aave}} l_{\text{pp}}} \right)^2 \tau_f l_{\text{fave}} \right)^2 + (\pi \mathcal{R}_{\text{ma}})^2 \right]^{1/2} \\ = \frac{1}{l_{\text{pp}}} \pi \mathcal{R}_{\text{ma}} (1 + \alpha^2)^{1/2}. \quad [12]$$

$I'_{\theta ap}$ can be expressed as:

$$I'_{\theta ap} = \Gamma \Phi_{\text{cpk}} \exp i (-\omega t + kz). \quad [13]$$

Note that Φ_{cpk} in the above equation is the constant, independent of time, t and space, z as defined by eq. [16] in the part-I, in which the infinitely long pump was discussed. In this part (part-III), the magnetic flux in the center core itself, Φ_c is not assumed as a simple periodic function of t and z to include the end effects so that $\Phi_c \neq \Phi_{\text{cpk}} \exp i (-\omega t + kz + \psi)$.

Eq. [8] can now be rearranged as:

$$\frac{\partial \Phi_c}{\partial t} = \frac{1}{1+w_i} \frac{l_{\text{fave}}}{\tau_f \sigma_f} \frac{\tau_x}{\mu_x l_{\text{aave}}} \frac{\partial^2 \Phi_c}{\partial z^2} - v_f \frac{\partial \Phi_c}{\partial z} + \frac{1}{1+w_i} \frac{l_{\text{fave}}}{\tau_f \sigma_f} \Gamma \Phi_{\text{cpk}} \exp i (-\omega t + kz). \quad [14]$$

By introducing:

$$D = \frac{1}{1+w_i} \frac{l_{\text{fave}}}{\tau_f \sigma_f} \frac{\tau_x}{\mu_x l_{\text{aave}}}, \quad [15]$$

$$N = v_f, \quad [16]$$

$$\Lambda = \frac{1}{1+w_i} \frac{l_{\text{fave}}}{\tau_f \sigma_f} \Gamma \Phi_{\text{cpk}}, \quad [17]$$

eq. [14] becomes a second order partial differential equation (PDE) for the magnetic flux, $\Phi_c(t, z)$ as:

$$\frac{\partial \Phi_c}{\partial t} = D \frac{\partial^2 \Phi_c}{\partial z^2} - N \frac{\partial \Phi_c}{\partial z} + \Lambda \exp i (-\omega t + kz), \quad [18]$$

which is mathematically same as a convection-diffusion equation with a periodic source term. Note that for the regions outside the pump where no applied current exist, $\Lambda = 0$ ($I'_{\theta ap} = 0$).

Solving the differential equation

By following the standard method to solve a PDE (such as Ref. 5), we assume that the magnetic flux in the center core has a form of:

$$\Phi_{c2}(t, z) = \Phi_{c2z}(z)\text{exp}i(-\omega t). \quad [19]$$

Substituting above equation into eq. [18] converts the PDE into an ordinary differential equation (ODE) for $\Phi_{c2z}(z)$ as:

$$D \frac{d^2 \Phi_{c2z}}{dz^2} - N \frac{\partial \Phi_{c2z}}{\partial z} + \omega i \Phi_{c2z} = -\Lambda \text{exp}i(kz). \quad [20]$$

First we obtain the homogeneous solution for the above ODE. The homogeneous ODE is:

$$D \frac{d^2 \Phi_{c2zh}}{dz^2} - N \frac{\partial \Phi_{c2zh}}{\partial z} + \omega i \Phi_{c2zh} = 0. \quad [21]$$

The characteristic equation is:

$$D\chi^2 - N\chi + \omega i = 0. \quad [22]$$

The solutions are given as:

$$\chi = \frac{N \pm \sqrt{N^2 - 4D\omega i}}{2D}, \quad [23]$$

or:

$$\chi = \frac{N \pm (P - Qi)}{2D}, \quad [24]$$

so that:

$$(P - Qi)^2 = N^2 - 4D\omega i, \quad [25]$$

which gives:

$$P^2 - Q^2 = N^2 > 0, \text{ and} \quad [26]$$

$$PQ = 2D\omega > 0. \quad [27]$$

By solving the above equations for P and Q , it follows that:

$$\chi_1 = \frac{N + (P - Qi)}{2D} \text{ and } \chi_2 = \frac{N - (P - Qi)}{2D}, \quad [28]$$

where:

$$P = \pm \left(\frac{\sqrt{N^4 + 4(2D\omega)^2 + N^2}}{2} \right)^{1/2}, \quad [29]$$

$$Q = \pm \left(\frac{\sqrt{N^4 + 4(2D\omega)^2 - N^2}}{2} \right)^{1/2}. \quad [30]$$

By inspecting these solutions, it is apparent that either positive or negative sign of eq. [29] and eq. [30] does not change the characteristics of eq. [28] (the solution requires that both need to be with the same sign from eq. [27] and $P > Q$ from eq. [26]). So we take the positive sign:

$$P = \left(\frac{\sqrt{N^4 + 4(2D\omega)^2 + N^2}}{2} \right)^{1/2}, \quad [31]$$

$$Q = \left(\frac{\sqrt{N^4 + 4(2D\omega)^2 - N^2}}{2} \right)^{1/2}. \quad [32]$$

The homogeneous solution is:

$$\Phi_{c2zh}(z) = c_{21}\exp(\chi_1 z) + c_{22}\exp(\chi_2 z). \quad [33]$$

Now we obtain the non-homogeneous solution for the ODE. The non-homogeneous ODE is:

$$D \frac{d^2 \Phi_{c2zn}}{dz^2} - N \frac{\partial \Phi_{c2zn}}{\partial z} + \omega i \Phi_{c2zn} = -\Lambda \exp i(kz). \quad [34]$$

A solution of the form of:

$$\Phi_{c2zn} = K \exp i(kz), \quad [35]$$

is assumed (Ref. 5). Substituting eq. [35] into eq. [34] yields:

$$K[Dk^2 + (kN - \omega)i] = \Lambda, \quad [36]$$

so the non-homogeneous solution is given as:

$$\Phi_{c2zn} = K \exp i(kz), \quad [37]$$

where:

$$K = \frac{\Lambda[Dk^2 + (kN - \omega)i]}{(Dk^2)^2 + (kN - \omega)^2}. \quad [38]$$

The solution for Φ_{c2z} is then given as:

$$\Phi_{c2z}(z) = c_{21}\exp(\chi_1 z) + c_{22}\exp(\chi_2 z) + K \exp i(kz), \quad [39]$$

and Φ_{c2} is:

$$\Phi_{c2}(t, z) = [c_{21}\exp(\chi_1 z) + c_{22}\exp(\chi_2 z) + K \exp i(kz)] \exp i(-\omega t), \quad [40]$$

where:

$$\chi_1 = \frac{N+(P-Qi)}{2D}, \quad [41]$$

$$\chi_2 = \frac{N-(P-Qi)}{2D}, \quad [42]$$

$$K = \frac{\Lambda[Dk^2+(kN-\omega)i]}{(Dk^2)^2+(kN-\omega)^2}, \quad [43]$$

and c_{21} and c_{22} are the constants of integration to be determined from the boundary conditions.

For outside the pump, $\Lambda = 0$. Also the magnetic structures do not exist outside the pump and we may assume that:

1. The relative effects of duct walls to the working fluid diminish, since the relative volume of the working fluid is larger than that of the duct wall outside the pump:

$$w_i \ll 1, \quad [44]$$

2. The air gap and the fluid thickness are considered equal, since all the volume inside the duct is occupied by the working fluid:

$$\tau_f \cong \tau_x, \quad [45]$$

3. Similarly, the circumference of the air gap and that of the fluid thickness are considered equal:

$$l_{fave} \cong l_{aave}, \quad [46]$$

so that:

$$D_o = \frac{1}{\mu_x \sigma_f}, \quad [47]$$

also depending on the cross sectional area of the duct outside the pump, the velocity of the working fluid outside the pump may be different from that inside the pump duct so that:

$$N_o = v_{fo}, \quad [48]$$

where subscript o indicates outside the pump. Now the PDE becomes:

$$\frac{\partial \Phi_c}{\partial t} = D_o \frac{\partial^2 \Phi_c}{\partial z^2} - N_o \frac{\partial \Phi_c}{\partial z}, \quad [49]$$

and a solution with a periodic boundary condition prescribed at $z = -\frac{1}{2}L_p$ for $z < -\frac{1}{2}L_p$ is given as (Ref. 6):

$$\Phi_{c1}(t, z) = c_1 \exp \left\{ \left(\frac{N_o}{2D_o} + \frac{P_o}{2D_o} \right) \left(z + \frac{1}{2}L_p \right) + i \left[-\omega t - \frac{Q_o}{2D_o} \left(z + \frac{1}{2}L_p \right) \right] \right\}$$

$$= c_1 \exp \left\{ \chi_{01} \left(z + \frac{1}{2} L_p \right) \right\} \exp i(-\omega t), \quad [50]$$

where:

$$P_0 = \left(\frac{\sqrt{N_0^4 + 4(2D_0\omega)^2 + N_0^2}}{2} \right)^{1/2}, \quad [51]$$

$$Q_0 = \left(\frac{\sqrt{N_0^4 + 4(2D_0\omega)^2 - N_0^2}}{2} \right)^{1/2}, \quad [52]$$

$$\chi_{01} = \frac{N_0 + (P_0 - Q_0 i)}{2D_0}, \quad [53]$$

which satisfies a periodic boundary condition of $c_1 \exp i(-\omega t)$ at $z = -\frac{1}{2} L_p$.

Another solution with a periodic boundary condition prescribed at $z = \frac{1}{2} L_p$ for $z > \frac{1}{2} L_p$ is given as:

$$\begin{aligned} \Phi_{c3}(t, z) &= c_3 \exp \left\{ \left(\frac{N_0}{2D_0} - \frac{P_0}{2D_0} \right) \left(z - \frac{1}{2} L_p \right) + i \left[-\omega t + \frac{Q_0}{2D_0} \left(z - \frac{1}{2} L_p \right) \right] \right\} \\ &= c_3 \exp \left\{ \chi_{02} \left(z - \frac{1}{2} L_p \right) \right\} \exp i(-\omega t), \end{aligned} \quad [54]$$

where:

$$\chi_{02} = \frac{N_0 - (P_0 - Q_0 i)}{2D_0}, \quad [55]$$

which satisfies a periodic boundary condition of $c_3 \exp i(-\omega t)$ at $z = \frac{1}{2} L_p$.

Now we have:

$$\Phi_{c1}(t, z) = c_1 \exp \left\{ \chi_{01} \left(z + \frac{1}{2} L_p \right) \right\} \exp i(-\omega t), \quad [56]$$

$$\Phi_{c2}(t, z) = [c_{21} \exp(\chi_1 z) + c_{22} \exp(\chi_2 z) + K \exp i(kz)] \exp i(-\omega t), \quad [57]$$

$$\Phi_{c3}(t, z) = c_3 \exp \left\{ \chi_{02} \left(z - \frac{1}{2} L_p \right) \right\} \exp i(-\omega t), \quad [58]$$

$$\frac{\partial}{\partial z} \Phi_{c1}(t, z) = c_1 \chi_{01} \exp \left\{ \chi_{01} \left(z + \frac{1}{2} L_p \right) \right\} \exp i(-\omega t), \quad [59]$$

$$\frac{\partial}{\partial z} \Phi_{c2}(t, z) = [c_{21} \chi_1 \exp(\chi_1 z) + c_{22} \chi_2 \exp(\chi_2 z) + K k i \exp i(kz)] \exp i(-\omega t), \quad [60]$$

$$\frac{\partial}{\partial z} \Phi_{c3}(t, z) = c_3 \chi_{02} \exp \left\{ \chi_{02} \left(z - \frac{1}{2} L_p \right) \right\} \exp i(-\omega t), \quad [61]$$

and $\Phi_{c1}(t, z)$ and $\Phi_{c2}(t, z)$, and $\frac{\partial}{\partial z} \Phi_{c1}(t, z)$ and $\frac{\partial}{\partial z} \Phi_{c2}(t, z)$ connect at $z = -\frac{1}{2}L_p$ and $\Phi_{c2}(t, z)$ and $\Phi_{c3}(t, z)$, and $\frac{\partial}{\partial z} \Phi_{c2}(t, z)$ and $\frac{\partial}{\partial z} \Phi_{c3}(t, z)$ connect at $z = \frac{1}{2}L_p$ with 4 unknowns, c_1 , c_{21} , c_{22} , and c_3 . The continuities of the spatial derivative of the magnetic flux is in fact the continuity of the radial magnetic flux density at the boundaries. The relationships are given as:

$$\Phi_{c1}\left(t, -\frac{1}{2}L_p\right) = \Phi_{c2}\left(t, -\frac{1}{2}L_p\right), \quad [62]$$

$$\Phi_{c2}\left(t, \frac{1}{2}L_p\right) = \Phi_{c3}\left(t, \frac{1}{2}L_p\right), \quad [63]$$

$$\frac{\partial}{\partial z} \Phi_{c1}\left(t, -\frac{1}{2}L_p\right) = \frac{\partial}{\partial z} \Phi_{c2}\left(t, -\frac{1}{2}L_p\right), \quad [64]$$

$$\frac{\partial}{\partial z} \Phi_{c2}\left(t, \frac{1}{2}L_p\right) = \frac{\partial}{\partial z} \Phi_{c3}\left(t, \frac{1}{2}L_p\right). \quad [65]$$

By solving these 4 equations, 4 unknowns, c_1 , c_{21} , c_{22} , and c_3 are determined as:

$$c_{21} = \frac{(\chi_{02}-\chi_2)(\chi_{01}-ki)\exp\left[\frac{1}{2}L_p(\chi_2-ki)\right] - (\chi_{01}-\chi_2)(\chi_{02}-ki)\exp\left[-\frac{1}{2}L_p(\chi_2-ki)\right]}{(\chi_{02}-\chi_1)(\chi_{01}-\chi_2)\exp\left[-\frac{1}{2}L_p(\chi_2-\chi_1)\right] - (\chi_{02}-\chi_2)(\chi_{01}-\chi_1)\exp\left[\frac{1}{2}L_p(\chi_2-\chi_1)\right]} K, \quad [66]$$

$$c_{22} = \frac{(\chi_{01}-\chi_1)(\chi_{02}-ki)\exp\left[-\frac{1}{2}L_p(\chi_1-ki)\right] - (\chi_{02}-\chi_1)(\chi_{01}-ki)\exp\left[\frac{1}{2}L_p(\chi_1-ki)\right]}{(\chi_{02}-\chi_1)(\chi_{01}-\chi_2)\exp\left[-\frac{1}{2}L_p(\chi_2-\chi_1)\right] - (\chi_{02}-\chi_2)(\chi_{01}-\chi_1)\exp\left[\frac{1}{2}L_p(\chi_2-\chi_1)\right]} K, \quad [67]$$

$$c_1 = c_{21}\exp\left(-\frac{1}{2}L_p\chi_1\right) + c_{22}\exp\left(-\frac{1}{2}L_p\chi_2\right) + K\exp\left(-\frac{1}{2}L_p k\right), \quad [68]$$

$$c_3 = c_{21}\exp\left(\frac{1}{2}L_p\chi_1\right) + c_{22}\exp\left(\frac{1}{2}L_p\chi_2\right) + K\exp\left(\frac{1}{2}L_p k\right). \quad [69]$$

From the magnetic flux, Φ_c , the radial magnetic fields strength, B_{ra} can be obtained from eq. [3], the induced current density in the working fluid, J_θ can also be obtained from eq. [4]. By substituting the expression for B_{ra} in \mathbf{B} and that of J_θ in \mathbf{j}_{ind} of eq. [60] of the part-I, an expression for the developed pressure gradient, $\frac{dP}{dz}$ may be obtained. The, using the first relationship shown in eq. [63] of the part-I, the developed pressure can be calculated by numerically integrating the developed pressure gradient.

Infinitely long pump case

For the infinitely long pump case, Φ_{c1} and Φ_{c3} do not exist. For Φ_{c2} to exist, $\lim_{L_p \rightarrow \infty} \Phi_{c2} = \Phi_{c2\infty} \neq \pm\infty$, which requires both c_{21} and c_{22} to be zero. As a result:

$$\Phi_{c2\infty}(t, z) = K\exp(-\omega t + kz). \quad [70]$$

By substituting eq. [38], this can be calculated as:

$$\Phi_{c2\infty} = \frac{\Lambda}{\sqrt{(Dk^2)^2 + (kN-\omega)^2}} \exp\left(-\omega t + kz - \arctan\left[\frac{kN-\omega}{Dk^2}\right]\right)$$

$$= \frac{\Lambda/(Dk^2)}{\sqrt{1+\left(\frac{\omega-kN}{Dk^2}\right)^2}} \expi\left(-\omega t + kz + \arctan\left[\frac{\omega-kN}{Dk^2}\right]\right) \quad [71]$$

Note that:

$$Dk^2 = \frac{1}{1+w_i} \frac{l_{fave}}{\tau_f \sigma_f} \frac{\tau_x}{\mu_x l_{aave}} \left(\frac{\pi}{l_{pp}}\right)^2 = \frac{k\Delta v}{\alpha} \frac{\mu_0}{\mu_x} \frac{\tau_x}{\tau_a} \frac{1}{C_{c2}}, \quad [72]$$

$$\omega - kN = \omega - v_f k = k\Delta v, \quad [73]$$

so that:

$$\frac{\omega-kN}{Dk^2} = C_{c2} \frac{\mu_x \tau_a}{\mu_0 \tau_x} \alpha, \quad [74]$$

and:

$$\Phi_{c2\infty} = \frac{1}{\mathcal{R}_{ma}} \frac{l_{pp}}{\pi} \frac{C_{c2} \frac{\mu_x \tau_a}{\mu_0 \tau_x}}{\sqrt{1+\left(C_{c2} \frac{\mu_x \tau_a}{\mu_0 \tau_x} \alpha\right)^2}} I'_{\theta_{appk}} \expi\left(-\omega t + kz + \arctan\left[C_{c2} \frac{\mu_x \tau_a}{\mu_0 \tau_x} \alpha\right]\right) \quad [75]$$

From eq. [16] of the part-I:

$$\Phi_c = \Phi_{cpk} \expi(-\omega t + kz + \psi), \quad [76]$$

and substitute eq. [31], eq. [9], eq. [10], and eq. [48], all from the part-I into the above equation:

$$\Phi_c = \frac{1}{\mathcal{R}_{ma}} \frac{l_{pp}}{\pi} \frac{1}{\sqrt{1+\alpha^2}} I'_{\theta_{appk}} \expi(-\omega t + kz + \arctan[\alpha]), \quad [77]$$

which is the equivalent expression for Φ_c from the part-I. By comparing the eq. [75] and eq. [77] above, it is clear that the method developed in the part-III to include the transport effects is consistent with the result from the part-I of the present work, which is only valid for the infinitely long pump case. Also in order to correctly reflect the effects represented by $C_{c2} \frac{\mu_x \tau_a}{\mu_0 \tau_x}$ (that is due to presence of multiple components in the air gap discussed earlier), $\mu_x = \mu_0$ and $\tau_x = C_{c2} \tau_a$.

References

5. E. Kreyszig, (1993) *Advanced engineering mathematics* 7th edition, John Wiley & Sons, Inc.
6. J. D. Logan and V. Zlotnik, (1995) "The convection-diffusion equation with periodic boundary conditions," *Appl. Math. Lett.*, vol. 8, No. 3, pp. 55-61.

Part-IV Calculation procedures

In the part-IV of the present work, procedures to design an ALIP and to calculate its performance using the model described in the part-I through part-III is explained.

Design calculation procedure

Input parameters

Net developed pressure: ΔP_n

Nominal flow rate: Q

Nominal slip: $s = \frac{v_s - v_f}{v_s}$

Pump length: L_p

Duct OD: OD_d

Duct wall thickness (outside) : t_{dO}

Duct wall thickness (inside) : t_{dI}

Gap between duct OD and stator ID: t_{dst}

Gap between core OD and core containment ID : t_{ccc}

Core allowable magnetic flux density: B_{cmax}

Stator allowable magnetic flux density: B_{stmax}

Core loss: W_{closs}

Number of poles: N_{poles}

Number of coils per pole per phase: N_{pppp}

Drive frequency: f_{dr}

Line-to-line voltage: V_{LL}

Number of layers of winding in a coil: $N_{coilayer}$

Coil allowable current density: $J_{coilmax}$

Calculating various major parameters

1. Pole pitch: $l_{pp} = \frac{L_p}{N_{poles}}$
2. Wave number: $k = \frac{\pi}{l_{pp}}$
3. Angular velocity: $\omega = 2\pi f_{dr}$
4. Synchronous velocity: $v_s = \frac{\omega}{k}$ Make sure it does not come too close to the maximum sodium velocity allowed.
5. Fluid velocity: $v_f = (1 - s)v_s$
6. Slip velocity: $\Delta v = v_s - v_f$

Determining the duct and air gap dimensions

7. Flow passage area: $A_f = \frac{Q}{v_f}$
8. Duct ID: $ID_d = OD_d - 2t_{dO}$
9. Core containment OD: $OD_{cc} = \sqrt{ID_d^2 - 4\frac{A_f}{\pi}}$
10. Core containment ID: $ID_{cc} = OD_{cc} - 2t_{dI}$
11. Core OD: $OD_c = ID_{cc} - 2t_{ccc}$
12. Stator ID: $ID_{st} = OD_d + 2t_{dst}$
13. Fluid thickness: $\tau_f = ID_d - OD_{cc}$
14. Average fluid diameter: $d_f = \frac{ID_d + OD_{cc}}{2}$
15. Average fluid circumference: $l_{fave} = \pi d_f$
16. Air gap thickness: $\tau_a = ID_{st} - OD_c$
17. Average air gap diameter: $d_a = \frac{ID_{st} - OD_c}{2}$
18. Average air gap circumference: $l_{aave} = \pi d_a$
19. Effective duct wall parameters: $\tau_w \sigma_w l_{wave}$
20. Duct wall factor: $w_i = \frac{\tau_w \sigma_w l_{fave} v_s}{\tau_f \sigma_f l_{wave} \Delta v}$ Part-I, eq. [39]

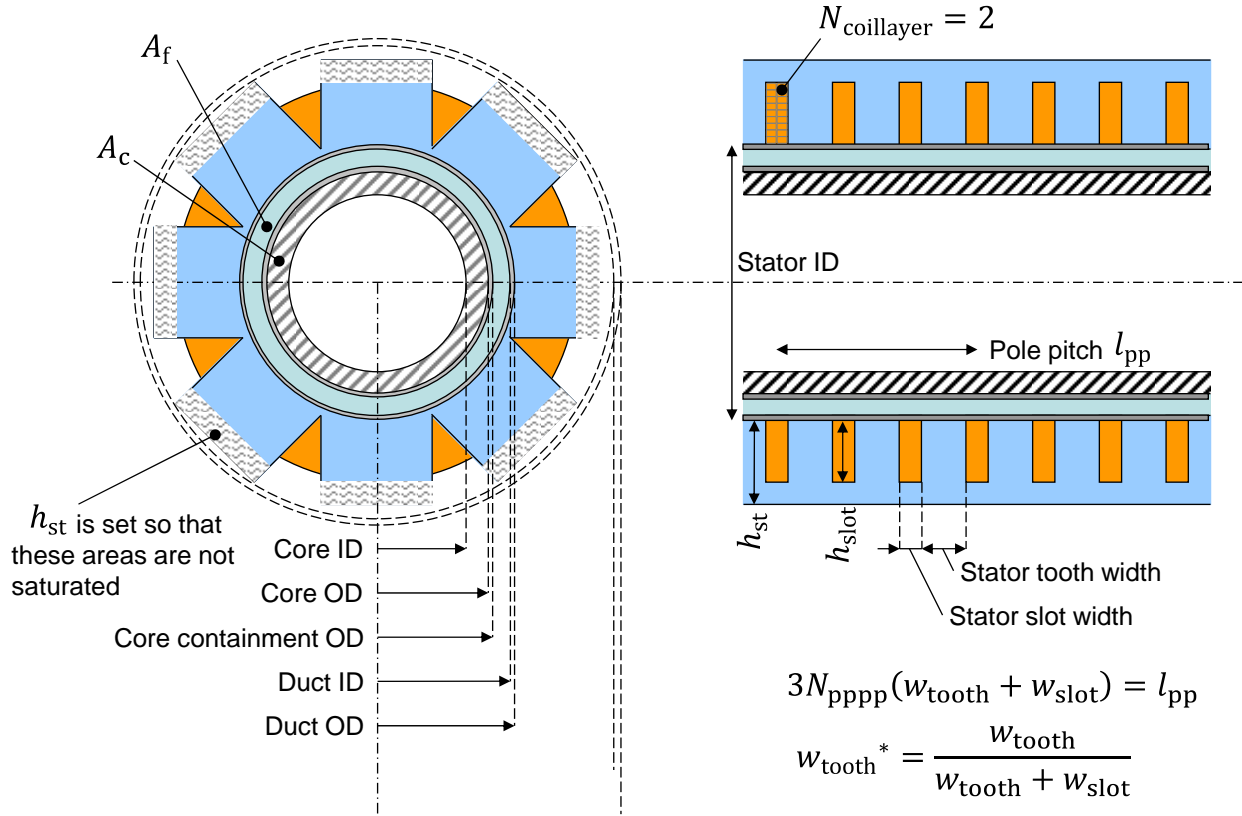


Figure 1. ALIP schematic image showing various parameters.

Determining the fluid dynamic pressure loss

21. Reynolds number: Re
22. Friction factor
23. Friction loss
24. Contraction loss
25. Expansion loss
26. Fluid dynamic pressure loss: ΔP_{loss}

Determining the actual applied voltage

27. Actual applied voltage per coil: $V_{\theta apact} = \frac{V_{LL}}{N_{poles}}$ Part-II, eq. [23]
28. Peak value for the actual applied voltage per coil: $V_{\theta apactpk} = \sqrt{2}V_{\theta apact}$

Adjustment in the developed pressure

29. Assign net developed pressure: ΔP_{ndev}
 - 29.1. Gross developed pressure: $\Delta P = \Delta P_{ndev} + \Delta P_{loss}$
 - 29.2. Developed pressure per pole: $\Delta P_{pp} = \frac{\Delta P}{N_{poles}}$

Calculating the peak magnetic field strength in the air gap and flux in the core

- 29.3. Peak radial magnetic flux density: $B_{\text{rapk}} = \sqrt{\frac{2\Delta P_{\text{pp}} l_{\text{fave}}}{l_{\text{pp}} \sigma_f \Delta v l_{\text{aave}}}}$ Part-I, eq. [63]
- 29.4. Peak magnetic flux in the center core: $\Phi_{\text{cpk}} = \frac{l_{\text{pp}}}{\pi} l_{\text{aave}} B_{\text{rapk}}$ Part-I, eq. [21]

Determining the core dimensions

- 29.5. Core cross sectional area: $A_c = \frac{\Phi_{\text{cpk}}}{B_{\text{cmax}}}$
- 29.6. Core ID: $ID_c = \sqrt{OD_c^2 - 4 \frac{A_c}{\pi}}$ Make sure the value exists, if not, stop calculation. Suggest increasing the pump duct diameter.

Determining the stator dimensions

- 29.7. Assign the initial stator tooth ratio: $w_{\text{tooth}}^* = 0.5$
- 29.7.1. Check if stator tooth is not saturated: $B_{\text{rapk}} < w_{\text{tooth}}^* \times B_{\text{stmax}}?$
If saturated, increase the tooth ratio until it is OK. If $w_{\text{tooth}}^* > w_{\text{tooth}}^*_{\text{max}}$, stop calculation. Suggest increasing the pump length.
- 29.7.2. Stator tooth width: $w_{\text{tooth}} = w_{\text{tooth}}^* \times \frac{l_{\text{pp}}}{3N_{\text{pppp}}}$
- 29.7.3. Stator slot width: $w_{\text{slot}} = \frac{l_{\text{pp}}}{3N_{\text{pppp}}} - w_{\text{tooth}}$

Calculating the magnetic reluctance of the air gap

- 29.7.4. Carter constant: C_{c1}
- 29.7.5. Carter coefficient: C_{c2}
- 29.7.6. Magnetic reluctance of the air gap: $\mathcal{R}_{ma} = \frac{\pi \tau_a \cdot C_{c2}}{\mu_0 \cdot l_{\text{pp}} l_{\text{aave}}}$ Part-I, eq. [29]

Calculating various electrical parameters

- 29.7.7. Factor: $\alpha = (1 + w_i) \frac{\tau_f \sigma_f}{l_{\text{fave}} \mathcal{R}_{ma}} \Delta v$ Part-I, eq. [49]
- 29.7.8. Factor: $\beta_c = \frac{\alpha}{\sqrt{1 + \alpha^2}}$ Part-I, eq. [48]
- 29.7.9. Phase angle: $\phi = -\arctan\left(\frac{1}{\alpha}\right)$ Part-I, eq. [52]
- 29.7.10. Phase angle: $\psi = \phi - \frac{\pi}{2}$ Part-I, eq. [44]
- 29.7.11. Conductor width: $w_{\text{cond}} = \frac{w_{\text{slot}}}{N_{\text{coillayer}}}$
- 29.7.12. Assign the initial core loss per pole: $W_{\text{closspp}} = 0$
- 29.7.12.1. Assign the initial peak value for the induced voltage per coil: $V_{\text{indpk}} = V_{\theta \text{apactpk}}$

Calculating the coil parameters

- 29.7.12.1.1. Number of turns per coil: $N_{\text{turns}} = \frac{V_{\text{indpk}}}{\omega \Phi_{\text{cpk}}}$ Part-II, eq. [8]
- 29.7.12.1.2. Current: $I_{\text{closspk}} = \frac{W_{\text{closspp}}}{3N_{\text{pppp}} \times \frac{1}{2} V_{\text{indpk}}}$ Part-II, eq. [6]
- 29.7.12.1.3. Current: $I_{\theta\text{coilpk}} = \frac{(1+w_i)^{\frac{1}{2}} l_{\text{pp}} \sigma_f \left(\frac{l_{\text{aave}}}{l_{\text{fave}}}\right)^2 \Delta v B_{\text{rapk}}^2 \tau_f l_{\text{fave}} v_s}{3N_{\text{pppp}} \times \frac{1}{2} V_{\text{indpk}}}$ Part-II, eq. [9]
- 29.7.12.1.4. Current: $I_{\theta\text{totpk}} = \frac{B_{\text{rapk}} \mathcal{R}_{\text{ma}} l_{\text{aave}} l_{\text{pp}}}{3 \times N_{\text{turns}} \times N_{\text{pppp}}}$ Part-II, eq. [11]
- 29.7.12.1.5. Phase angle: $\xi = -\tan\left(\frac{I_{\theta\text{totpk}}}{I_{\theta\text{coilpk}} + I_{\text{closspk}}}\right)$ Part-II, eq. [14]
- 29.7.12.1.6. Phase angle: $\Delta\theta_1 = \xi - \psi + \frac{\pi}{2}$ Part-II, eq. [15]
- 29.7.12.1.7. Current: $I_{\theta\text{apactpk}} = \sqrt{(I_{\theta\text{coilpk}} + I_{\text{closspk}})^2 + I_{\theta\text{totpk}}^2}$ Part-II, eq. [16]
- 29.7.12.1.8. Conductor cross sectional area: $S_{\text{cond}} = \frac{I_{\theta\text{apactpk}}}{J_{\text{coilmax}}}$
- 29.7.12.1.9. Conductor height: $h_{\text{cond}} = \frac{S_{\text{cond}}}{w_{\text{cond}}}$
- 29.7.12.1.10. Coil resistance from the geometry: R_{pri}
- 29.7.12.1.11. Coil reactance from the geometry: X_{pri}
- 29.7.12.1.12. Phase angle: $\Delta\theta_2 = \arctan\left(\frac{V_{\text{indpk}} \sin \xi - I_{\theta\text{apactpk}} X_{\text{pri}}}{V_{\text{indpk}} \cos \xi + I_{\theta\text{apactpk}} R_{\text{pri}}}\right) - \xi$ Part-II, eq. [20]
- 29.7.12.1.13. Back-calculate the peak value for the induced voltage per coil: V_{indpk} from $V_{\theta\text{apactpk}}$ Part-II, eq. [18]
- 29.7.12.1.14. Check if V_{indpk} is converged. If not, go back to step 29.7.12.1.1
- 29.7.12.2. Slot opening area: $S_{\text{slot}} = S_{\text{cond}} N_{\text{turns}}$
- 29.7.12.3. Slot opening height: $h_{\text{slot}} = \frac{S_{\text{slot}}}{w_{\text{slot}}}$
- 29.7.12.4. Stator height: $h_{\text{st}} = \frac{\Phi_{\text{cpk}}}{B_{\text{stmax}}} \times \frac{1}{\pi I D_{\text{st}}} + h_{\text{slot}}$
- 29.7.12.5. Calculate the core loss per pole: $W_{\text{closspp}} = f(W_{\text{closs}})$
- 29.7.12.6. Check if W_{closspp} is converged. If not, go back to step 29.7.12.1.1

Calculating the overall pump size

- 29.7.13. Overall pump diameter:

Calculating the overall pump efficiency

- 29.7.14. Power per coil: $P_{\text{coilre}} = \frac{1}{2} V_{\theta\text{apactpk}} I_{\theta\text{apactpk}} \cos(\xi + \Delta\theta_2)$
- 29.7.15. Total power input: $P_p = 3N_{\text{pppp}} N_{\text{poles}} P_{\text{coilre}}$
- 29.7.16. Efficiency: $\eta_p = \frac{\Delta P_n Q}{P_p}$
- 29.7.17. Check if η_p is maximum. If maximum, go to 29.8, if not, modify the stator tooth ratio: w_{tooth}^* .
- 29.7.18. Check if w_{tooth}^* is in the good range (ex: 0.25-0.75). If OK, go back to step 29.7.1, if not, go to 29.8.
- 29.8. Total phase current: $I_p = \frac{I_{\theta\text{apactpk}}}{\sqrt{2}} N_{\text{pppp}}$ Part-II, eq. [24].
- 29.9. Phase angle: $\xi + \Delta\theta_2$.

Calculating the end effect

- 29.10. Coefficient: $\Gamma = \frac{1}{l_{\text{pp}}} \pi \mathcal{R}_{\text{ma}} (1 + \alpha^2)^{1/2}$ Part-III, eq. [12].
- 29.11. Coefficient: $D = \frac{1}{1+w_i} \frac{l_{\text{fave}} \tau_x}{\tau_f \sigma_f \mu_x l_{\text{aave}}}$ Part-III, eq. [15].
- 29.12. Coefficient: $N = v_f$ Part-III, eq. [16].
- 29.13. Coefficient: $\Lambda = \frac{1}{1+w_i} \frac{l_{\text{fave}}}{\tau_f \sigma_f} \Gamma \Phi_{\text{cpk}}$, Part-III, eq. [17].
- 29.14. Coefficient: $P = \left(\frac{\sqrt{N^4 + 4(2D\omega)^2} + N^2}{2} \right)^{1/2}$, Part-III, eq. [31].
- 29.15. Coefficient: $Q = \left(\frac{\sqrt{N^4 + 4(2D\omega)^2} - N^2}{2} \right)^{1/2}$ Part-III, eq. [32].
- 29.16. Coefficient: $\chi_1 = \frac{N + (P - Qi)}{2D}$ Part-III, eq. [28].
- 29.17. Coefficient: $\chi_2 = \frac{N - (P - Qi)}{2D}$ Part-III, eq. [28].
- 29.18. Coefficient: $K = \frac{\Lambda [Dk^2 + (kN - \omega)i]}{(Dk^2)^2 + (kN - \omega)^2}$ Part-III, eq. [38].
- 29.19. Constants: c_1, c_{21}, c_{22} , and c_3 : Part-III, eqs. [66]-[69]
- 29.20. Axial magnetic flux distribution: Φ_c
- 29.21. Radial magnetic flux distribution: B_{ra} Part-III, eq. [3]
- 29.22. Circumferential induced current density distribution: J_θ Part-III, eq. [4]
- 29.23. Developed pressure gradient: $\frac{dP}{dz}$ Part-I, eq. [60]
- 29.24. New gross developed pressure including the end effect: ΔP_{gdev} From numerical integration of $\frac{dP}{dz}$
- 29.25. Update the net developed pressure: $\Delta P_{\text{ndev}} = \Delta P_{\text{gdev}} - \Delta P_{\text{loss}}$
- 29.26. Check if $\Delta P_n = \Delta P_{\text{ndev}}$ is achieved. If not, $\Delta P_{\text{ndev}} = \Delta P_{\text{ndev}} + (\Delta P_n - \Delta P_{\text{ndev}})$ and go back to step 29.1.
30. End of calculation.

Performance calculation procedure

Input parameters

Nominal flow rate: Q

Pump length: L_p

Duct OD: OD_d

Duct wall thickness (outside) : t_{dO}

Duct wall thickness (inside) : t_{dI}

Gap between duct OD and stator ID: t_{dst}

Gap between core OD and core containment ID : t_{ccc}

Core allowable magnetic flux density: B_{cmax}

Stator allowable magnetic flux density: B_{stmax}

Core loss: W_{closs}

Number of poles: N_{poles}

Number of coils per pole per phase: N_{pppp}

Drive frequency: f_{dr}

Line-to-line voltage: V_{LL}

Number of layers of winding in a coil: $N_{coilayer}$

Coil allowable current density: $J_{coilmax}$

Calculating various major parameters

1. Pole pitch: $l_{pp} = \frac{L_p}{N_{poles}}$
2. Wave number: $k = \frac{\pi}{l_{pp}}$
3. Angular velocity: $\omega = 2\pi f_{dr}$
4. Synchronous velocity: $v_s = \frac{\omega}{k}$ Make sure it does not come too close to the maximum sodium velocity allowed.
5. Flow passage area: $A_f = \frac{\pi}{4}(ID_d^2 - OD_{cc}^2)$
6. Fluid velocity: $v_f = \frac{Q}{A_f}$

7. Slip velocity: $\Delta v = v_s - v_f$

Calculate the duct and air gap dimensions

8. Duct ID: $ID_d = OD_d - 2t_{dO}$
9. Core containment OD: OD_{cc} Given
10. Core containment ID: $ID_{cc} = OD_{cc} - 2t_{dI}$
11. Core OD: $OD_c = ID_{cc} - 2t_{ccc}$
12. Stator ID: $ID_{st} = OD_d + 2t_{dst}$
13. Fluid thickness: $\tau_f = ID_d - OD_{cc}$
14. Average fluid diameter: $d_f = \frac{ID_d + OD_{cc}}{2}$
15. Average fluid circumference: $l_{fave} = \pi d_f$
16. Air gap thickness: $\tau_a = ID_{st} - OD_c$
17. Average air gap diameter: $d_a = \frac{ID_{st} - OD_c}{2}$
18. Average air gap circumference: $l_{aave} = \pi d_a$
19. Effective duct wall parameters: $\tau_w \sigma_w l_{wave}$
20. Duct wall factor: $w_i = \frac{\tau_w \sigma_w l_{fave} v_s}{\tau_f \sigma_f l_{wave} \Delta v}$ Part-I, eq. [39]
21. Core ID: $ID_c = \sqrt{OD_c^2 - 4 \frac{A_c}{\pi}}$

Calculate the stator dimensions

22. Stator tooth width: $w_{tooth} = w_{tooth}^* \times \frac{l_{pp}}{3N_{pppp}}$
23. Stator slot width: $w_{slot} = \frac{l_{pp}}{3N_{pppp}} - w_{tooth}$
24. Slot opening height: $h_{slot} = \frac{S_{slot}}{w_{slot}}$
25. Stator height: $h_{st} = \frac{\Phi_{cpk}}{B_{stmax}} \times \frac{1}{\pi ID_{st}^2} + h_{slot}$

Calculate the coil parameters

26. Conductor width: $w_{cond} = \frac{w_{slot}}{N_{coillayer}}$
27. Conductor height: $h_{cond} = \frac{S_{cond}}{w_{cond}}$
28. Coil resistance from the geometry: R_{pri}
29. Coil reactance from the geometry: X_{pri}
30. Core loss per pole: $W_{closspp} = f(W_{closs})$

Calculate the fluid dynamic pressure loss

31. Reynolds number: Re
32. Friction factor

33. Friction loss
34. Contraction loss
35. Expansion loss
36. Fluid dynamic pressure loss: ΔP_{loss}

Calculate some parameters

37. Carter constant: C_{c1}
38. Carter coefficient: C_{c2}
39. Magnetic reluctance of the air gap: $\mathcal{R}_{ma} = \frac{\pi \tau_a \cdot C_{c2}}{\mu_0 \cdot l_{pp} l_{aave}}$ Part-I, eq. [29]
40. Factor: $\alpha = (1 + w_i) \frac{\tau_f \sigma_f}{l_{fave} \mathcal{R}_{ma}} \Delta v$ Part-I, eq. [49]
41. Factor: $\beta_c = \frac{\alpha}{\sqrt{1+\alpha^2}}$ Part-I, eq. [48]
42. Phase angle: $\phi = -\arctan\left(\frac{1}{\alpha}\right)$ Part-I, eq. [52]
43. Phase angle: $\psi = \phi - \frac{\pi}{2}$ Part-I, eq. [44]
44. Actual applied voltage per coil: $V_{\theta\text{apact}} = \frac{V_{LL}}{N_{\text{poles}}}$ Part-II, eq. [23]
45. Peak value for the actual applied voltage per coil: $V_{\theta\text{apactpk}} = \sqrt{2} V_{\theta\text{apact}}$

Determine the electrical parameters

46. Assign the initial peak value for the induced voltage per coil: $V_{\text{indpk}} = V_{\theta\text{apactpk}}$
- 46.1. Peak magnetic flux in the center core: $\Phi_{\text{cpk}} = \frac{V_{\text{indpk}}}{\omega N_{\text{turns}}}$ Part-II, eq. [8]
- 46.2. Peak radial magnetic flux density: $B_{\text{rapk}} = \frac{1}{l_{aave}} \frac{\pi}{l_{pp}} \Phi_{\text{cpk}}$ Part-I, eq. [20]
- 46.3. Check if stator is not saturated: $\pi I D_{\text{st}} (h_{\text{st}} - h_{\text{slot}}) > \frac{\Phi_{\text{cpk}}}{B_{\text{stmax}}}$ If saturated, stop calculation.
- 46.4. Check if stator tooth is not saturated: $B_{\text{rapk}} < w_{\text{tooth}}^* \times B_{\text{stmax}}$ If saturated, stop calculation.
- 46.5. Check if core is not saturated: $A_c > \frac{\Phi_{\text{cpk}}}{B_{\text{cmax}}}$

Determine the actual developed pressure

- 46.6. Developed pressure per pole: $\Delta P_{\text{pp}} = \frac{1}{2} l_{pp} \sigma_f \frac{l_{aave}}{l_{fave}} \Delta v B_{\text{rapk}}^2$ Part-I, eq. [63]
- 46.7. Gross developed pressure: $\Delta P = N_{\text{poles}} \Delta P_{\text{pp}}$
- 46.8. Net developed pressure: $\Delta P_n = \Delta P - \Delta P_{\text{loss}}$
- 46.9. Current: $I_{\text{closspk}} = \frac{W_{\text{closspp}}}{3 N_{\text{pppp}} \times \frac{1}{2} V_{\text{indpk}}}$ Part-II, eq. [6]
- 46.10. Current: $I_{\theta\text{coilpk}} = \frac{(1+w_i) \frac{1}{2} l_{pp} \sigma_f \left(\frac{l_{aave}}{l_{fave}}\right)^2 \Delta v B_{\text{rapk}}^2 \tau_f l_{fave} v_s}{3 N_{\text{pppp}} \times \frac{1}{2} V_{\text{indpk}}}$ Part-II, eq. [9]

- 46.11. Current: $I_{\theta\text{totpk}} = \frac{B_{\text{rapk}} \mathcal{R}_{\text{ma}} l_{\text{aave}} l_{\text{pp}}}{3 \times N_{\text{turns}} \times N_{\text{pppp}}}$ Part-II, eq. [11]
- 46.12. Phase angle: $\xi = -\tan\left(\frac{I_{\theta\text{totpk}}}{I_{\theta\text{coilpk}} + I_{\text{closspk}}}\right)$ Part-II, eq. [14]
- 46.13. Phase angle: $\Delta\theta_1 = \xi - \psi + \frac{\pi}{2}$ Part-II, eq. [15]
- 46.14. Current: $I_{\theta\text{apactpk}} = \sqrt{(I_{\theta\text{coilpk}} + I_{\text{closspk}})^2 + I_{\theta\text{totpk}}^2}$ Part-II, eq. [16]
- 46.15. Phase angle: $\Delta\theta_2 = \arctan\left(\frac{V_{\text{indpk}} \sin\xi - I_{\theta\text{apactpk}} X_{\text{pri}}}{V_{\text{indpk}} \cos\xi + I_{\theta\text{apactpk}} R_{\text{pri}}}\right) - \xi$ Part-II, eq. [20]
- 46.16. Back-calculate the peak value for the induced voltage per coil: V_{indpk} from $V_{\theta\text{apactpk}}$ Part-II, eq. [18]
- 46.17. Check if V_{indpk} is converged. If not, go back to step 46.1

Calculating the overall pump size

47. Overall pump diameter:

Calculating the overall pump efficiency

48. Power per coil: $P_{\text{coilre}} = \frac{1}{2} V_{\theta\text{apactpk}} I_{\theta\text{apactpk}} \cos(\xi + \Delta\theta_2)$
49. Total power input: $P_{\text{p}} = 3 N_{\text{pppp}} N_{\text{poles}} P_{\text{coilre}}$
50. Total phase current: $I_{\text{p}} = \frac{I_{\theta\text{apactpk}}}{\sqrt{2}} N_{\text{pppp}}$ Part-II, eq. [24].
51. Phase angle: $\xi + \Delta\theta_2$.
52. Efficiency: $\eta_{\text{p}} = \frac{\Delta P_{\text{n}} Q}{P_{\text{p}}}$

Calculating the end effect

53. Coefficient: $\Gamma = \frac{1}{l_{\text{pp}}} \pi \mathcal{R}_{\text{ma}} (1 + \alpha^2)^{1/2}$ Part-III, eq. [12].
54. Coefficient: $D = \frac{1}{1 + w_i} \frac{l_{\text{fave}} \tau_x}{\tau_f \sigma_f \mu_x l_{\text{aave}}}$ Part-III, eq. [15].
55. Coefficient: $N = v_f$ Part-III, eq. [16].
56. Coefficient: $\Lambda = \frac{1}{1 + w_i} \frac{l_{\text{fave}}}{\tau_f \sigma_f} \Gamma \Phi_{\text{cpk}}$ Part-III, eq. [17].
57. Coefficient: $P = \left(\frac{\sqrt{N^4 + 4(2D\omega)^2} + N^2}{2}\right)^{1/2}$, Part-III, eq. [31].
58. Coefficient: $Q = \left(\frac{\sqrt{N^4 + 4(2D\omega)^2} - N^2}{2}\right)^{1/2}$ Part-III, eq. [32].
59. Coefficient: $\chi_1 = \frac{N + (P - Qi)}{2D}$ Part-III, eq. [28].
60. Coefficient: $\chi_2 = \frac{N - (P - Qi)}{2D}$ Part-III, eq. [28].
61. Coefficient: $K = \frac{\Lambda [Dk^2 + (kN - \omega)i]}{(Dk^2)^2 + (kN - \omega)^2}$ Part-III, eq. [38].

62. Constants: $c_1, c_{21}, c_{22},$ and c_3 : Part-III, eqs. [66]-[69]
63. Axial magnetic flux distribution: Φ_c
64. Radial magnetic flux distribution: B_{ra} Part-III, eq. [3]
65. Circumferential induced current density distribution: J_θ Part-III, eq. [4]
66. Developed pressure gradient: $\frac{dP}{dz}$ Part-I, eq. [60]
67. Gross developed pressure including the end effect: ΔP_{gdev} From numerical integration of $\frac{dP}{dz}$
68. Net developed pressure: $\Delta P_n = \Delta P_{gdev} - \Delta P_{loss}$
69. End of calculation.



Nuclear Engineering Division

Argonne National Laboratory
9700 South Cass Avenue, Bldg. 362
Argonne, IL 60439

www.anl.gov



Argonne National Laboratory is a U.S. Department of Energy
laboratory managed by UChicago Argonne, LLC